EDWARD UCHECHUKWU IWUCHUKWU

Stochastic Modelling And Simulation of Free Radical Polymerization of Styrene in Microchannels using a hybrid Gillespie Algorithm

São Paulo
2024

EDWARD UCHECHUKWU IWUCHUKWU

Stochastic Modelling And Simulation of Free Radical Polymerization of Styrene in Microchannels using a hybrid Gillespie Algorithm

Versão Corrigida

Dissertação apresentada à Escola Politécnica da Universidade de São Paulo para obtenção do Título de Mestre em Ciências.

Área de Concentração:

Engenharia Química

Orientador:

Prof. Dr. Ardson dos Santos Vianna Junior

São Paulo
2024

Este exemplar foi revisado e corrigido em relação à versão original, sob responsabilidade única do autor e com a anuência de seu orientador.

São Paulo, _____ de _____ de _____

Assinatura do autor: _____

Assinatura do orientador: _____

Catalogação-na-publicação

Iwuchukwu, Edward Uchechukwu
Modelagem estocástica e simulação da polimerização radicalar livre de estireno em microcanais usando um algoritmo híbrido de Gillespie / E. U. Iwuchukwu -- versão corr. -- São Paulo, 2024.
95 p.

Dissertação (Mestrado) - Escola Politécnica da Universidade de São Paulo. Departamento de Engenharia Química.

1.Polimerização 2.Algoritmo de simulação estocástica 3..Intensificação de processos I.Universidade de São Paulo. Escola Politécnica. Departamento de Engenharia Química II.t.

Acknowledgements

First of all, I want to thank God almighty for His unwavering grace, blessings and provisions towards me during the course of this chapter in my life. In addition, I would like to appreciate the support and prayers of my parents as well as my extended family for their love and support.

Also, I would like to thank my academic advisor Prof. Dr. Ardson dos Santos Vianna Junior for the opportunity to carry out my master's degree program under his supervision and for the experience and learning during this time.

Also, I appreciate the helpful academic inputs and suggestions of Prof. Dr. Adriano Francisco Siqueira of the School of Engineering, Lorena (USP), Prof. Dr. Caroline Satye Nakama of the Norwegian University of Science and Technology, Norway and, Prof. Dr. Martina Costa Reis of the Polytechnic School, University of Sao Paulo (PEQ-EPUSP/PQI) during my qualification examination and final thesis defence.

Finally, I want to appreciate the kindness and support of Paulo, Micheal, Patience, Taofeeq and Gustavo at the various stages of the program and other colleagues, academic and non-academic staff at the department (PEQ-EPUSP/PQI) who contributed towards the success of my master's degree program.

This study was financed in part by the Coordenação de Aperfeiçoamento de Pessoal de Nível Superior - Brasil (CAPES) - Finance Code 001.

It is the glory of God to conceal a matter,
But the glory of kings is to search out a matter.
(Holy Bible, Proverbs 25:2)

RESUMO

Recentemente, foram conduzidos estudos avançados sobre a produção de poliestireno através da polimerização via radicais livres (FRP) em microcanais. Esse tema tem despertado grande interesse, principalmente devido à eficiência proporcionada pelos microrreatores em termos de intensificação do processo. Além disso, especialmente em plantas-piloto, os microrreatores têm sido utilizados devido à sua eficácia no monitoramento das características ou propriedades finais do polímero poliestireno, que variam conforme o tamanho da cadeia polimérica. Por outro lado, um problema crítico encontrado em microrreatores e milirreatores é o entupimento dos microcanais.

Neste trabalho, foi simulada a síntese de poliestireno via FRP em microcanal utilizando um algoritmo robusto e eficiente em termos de tempo, baseado na simulação estocástica híbrida baseada no algoritmo de Gillespie. Esse método não apenas simula o crescimento da cadeia polimérica, mas também permite um cálculo determinístico paralelo simultâneo do mesmo sistema de reação. Os perfis determinísticos obtidos em diferentes condições foram comparados com as respectivas trajetórias estocásticas.

Para validar o modelo, os resultados obtidos para a conversão de monômero (X), o índice de polidispersidade (PDI), o peso molecular médio numérico (Mn) e o peso molecular médio ponderado (Mw) foram comparados aos dados experimentais. Foram utilizados tempos de residência variando de 5 a 80 minutos e diferentes condições operacionais, incluindo concentrações iniciais de monômero (M), solvente (S) e iniciador (I) e, também, temperaturas variando entre 100 e 140 graus Celsius.

O erro percentual médio (APE - Average Percentage Error) obtido a partir da simulação determinística pelo algoritmo de simulação estocástica híbrida ($HSSA$) aproxima-se dos resultados encontrados na literatura, validando assim a capacidade de simular a polimerização via FRP do monômero de estireno. Dessa forma, aplicando diferentes condições de entrada, o algoritmo foi utilizado para prever simultaneamente os perfis determinísticos e as trajetórias estocásticas. O modelo estocástico permite a compreensão dos fenômenos físicos que ocorrem dentro de um microrreator.

Palavras-Chave – Poliestireno, Microcanais, Algoritmo de Simulação Estocástica Híbrida, Algoritmo Gillespie, Polimerização via Radicais Livres, Intensificação de Processos.

ABSTRACT

Most recently, advanced studies have been carried out on the production of polystyrene by Free Radical Polymerization (FRP) via microchannels. This has been a subject of core interest primarily due to the efficiency of a microreactor in terms of process intensification. In addition, especially in pilot experimentations, a micro or milli-reactor has been known widely to be efficient in monitoring the microstructural end-use features or properties of the polystyrene polymer as the chain grows and ultimately terminates. However, a critical problem that occurs in milli- and micro-reactors is the clogging of the microchannels.

In this work, the synthesis of polystyrene via FRP through microchannels is simulated using a robust and time-efficient Hybrid Stochastic Simulation Algorithm based on the Gillespie Algorithm. This algorithm not only simulates the chain growth polymerization but also allows a simultaneous parallel deterministic computation of the same chain growth reaction system. The produced deterministic profiles at various conditions were compared to the respective stochastic trajectories.

To validate the model, the obtained results of the end-use properties of polystyrene such as Monomer Conversion (X), Polydispersity Index (PDI), Number-Average Molar Mass (Mn) and Weight-Average Molar Mass (Mw) were compared to experimental data. Also, the residence times deployed for the simulation was from 5 to 80 minutes and as well as varying operating conditions of initial Monomer (M), Solvent (S) and Initiator (I) which includes temperatures ranging from 100 and 140 degrees Celsius.

The Average Percentage Error (APE) obtained from the deterministic simulation of the hybrid stochastic simulation algorithm ($HSSA$) was close to the results found in literature, thus validating the efficiency of the algorithm to simulate the polymerization via FRP of the styrene monomer. Thus, applying different input conditions, the algorithm was used to simultaneously predict deterministic profiles and stochastic trajectories. The stochastic model allows us to understand the physical phenomena that occur inside a microreactor.

Keywords – Polystyrene, Microchannels, Hybrid Stochastic Simulation Algorithm, Gillespie Algorithm, Free Radical Polymerization, Process Intensification.

LIST OF FIGURES

LIST OF TABLES

LIST OF ABBREVIATIONS

ATRP	Atom transfer radical polymerization
APE	Average Percentage Error
BP	Biodegradable polymers
CFPE	Chemical Fokker-Planck equation
CP	Conductive Polymers
CLD	Chain Length Distribution
CLE	Chemical Langevin Equation
CLM	Chemical Langevin Method
CKE	Chapman - Kolmogorov Equation
CME	Chemical Master Equation
CRP	Controlled Radical Polymerization
DAE	Differential Algebraic Equation
DM	Direct Method
DSM	Deterministic Simulation Method
FRM	First Reaction Method
FRP	Free Radical Polymerization
GA	Gillespie Algorithm
GRP	Graphene-reinforced polymers
HSSA	Hybrid Stochastic Simulation Algorithm
HSNN	Hybrid Stochastic Neural Network
RRE	Rate Reaction Equation
KMC	Kinetic Monte Carlo
LCA	Long Chain Approximation
MMA	Methyl Methacrylate
MWD	Molecular Weight Distribution
MCM	Monte Carlo Method

NRM	Next Reaction Method
NN	Neural Network
ODE	Ordinary Differential Equation
PSD	Particle Size Distribution
PRD	Poisson Random Distribution
PDI	Polydispersity Index
PSSH	Pseudo Steady-State Hypothesis
QSSA	Quasi-Steady State Approximation
RP	Radical polymerization
RAFT	Reversible Addition-Fragmentation Chain-Transfer Polymerization
RRE	Rate Reaction Equation
RBM	Rejection Based Method
RSME	Root Mean Square Error
SDE	Stochastic Differential Equation
SHP	Self-Healing Polymers
SMP	Shape-Memory Polymers
SFRP	Stable Free Radical Polymerization
SRP	Stimuli-Responsive Polymers
SSA	Stochastic Simulation Algorithm
URD	Uniform Random Distribution

LIST OF SYMBOLS

$D^{\bullet}$	Dead polymer concentration
I	Initiator concentration
f	Initiator efficiency
K_I	Kinetic constant for chain initiation
K_P	Kinetic constant for chain propagation
K_{tc}	Kinetic constant for chain termination by combination
K_{td}	Kinetic constant for chain termination by disproportionation
K_{trM}	Kinetic constant for chain transfer to monomer
K_{trS}	Kinetic constant for chain transfer to solvent
K_d	Kinetic constant for initiator dissociation
K_{iterm}	Kinetic constant for thermal initiation
$P^{\bullet}$	Live polymer
X_i	State of Molecular Specie
M	Monomer concentration
X	Monomer conversion
M_n	Number-average molar mass
N_A	Avogrado Number
h_j	Number of reaction combinations
T	Operating temperature
$R^{\bullet}$	Radical concentration
β	Rate of polymerization
R_j	Reaction channel
α_j	Reaction propensity
V	Reaction volume
t	Simulation or residence time
S_i	Molecular Specie

s_i	Number of molecular Species
S	Solvent concentration
v_{ij}	State change vector
c_j	Stochastic constant
τ	Time interval or Leap
R	Universal gas constant
M_w	Weight-average molar mass
Z_j	Independent normal random variable

TABLE OF CONTENTS

CHAPTER 1
INTRODUCTION

In recent years, the synthesis of polystyrene via Free Radical Polymerization (FRP) in microchannels probes into the increasing level of macromolecular details and the characterization of the polymer's microstructure. (DAGMAR et al., 2016) One of the pivotal applications of the micro- or milli-reactor technology is that it bridges the gap between the synthesis of the end-use features of the polymer at the microscale and macroscale. In other words, at the mesoscale, the fundamental polymer's final characteristics are described in terms of Particle Size Distribution (PSD) hence, the information obtained is then used to make informed decisions regarding the interaction between the micro- and macro-scale of the Free Radical Polymerization (FRP) reaction system. (DAGMAR et al., 2016)

Also, polymer engineers have been on a quest to utilize continuous flow processes in microchannels to improve polystyrene's quality in terms high reproducible molecular weight distribution and improved overall productivity. (VIANNA Jr. et al., 2007) Vianna Jr. (2003) investigated the polymerization of styrene in tubular reactors, he observed perturbations contributed by stochastic noise resulting from varying feeding mechanisms in conventional tubular reactors. Also, it was observed in the investigation that stochastic noise effects of the fluid dynamics in tubular reactors for the polystyrene synthesis could not be entirely determined by traditional deterministic simulation approaches. (VIANNA JR., 2003)

From a microscopic perspective, an ensemble of the stochastic trajectories obtained within the bounds of statistical confidence can be referenced to predict the key features of the polymer as feeding conditions are varied during the polymerization at a pilot experimentation level. (Martin and Audus, 2023; D.T. GILLESPIE, 2007) In addition, the reproducibility of the simulation results or outcomes at small scales is very important in order to improve the polymer's end-use properties hence, the Stochastic Simulation Algorithm (SSA) employed in this case. This choice of investigation is predicated on factors affecting complex chemical reaction systems such as FRP reaction system : (**I**) Impact of polymerization computation and analysis, (**II**) the validity of experimental

and published kinetics values in literature, (**III**) industrial challenges, and (**IV**) choice of computational algorithm . (GARTNER and JAYARAMAN, 2019; MEIMAROGLOU and KIPARISSIDES, 2014)

This project probes the significant issues in FRP of Styrene by combining the application of stochastic simulation and a deterministic approach to simulate the rate of formation of polystyrene in microchannels (milli-reactor). The SSA technique finds its foundation in the Chemical Master Equation (CME) which is intractable to simulate deterministically when considering complex chemical reactions. (D.T. GILLESPIE, 1976) Also, the stochastic perturbation of a dynamic chemical reaction system is latent at small molecular copy numbers for a chain growth polymerization systems. The application of the proposed Hybrid Stochastic Simulation Algorithm (HSSA) used in this investigation was carried out at different initial feeding conditions or formulations for the monomer (M), solvent (S), and initiator (I) at different molar quantities as well as the varying operating temperatures. The chemical and thermal initiation reaction of the kinetics of the Free Radical Polymerization (FRP) of Styrene was considered in different instances under the prevailing defined conditions. Thus, one can compare the stochastic and corresponding deterministic profiles at volumes mimicking that of a micro- or milli-reactor. Subsequently, a cursory look into different techniques employed to simulate the FRP of styrene over the years will be revised.

1.1 Context and Motivation

Extensive research has been carried out in order to improve the end-use properties of polymeric materials by controlling the polymer's microstructure during synthesis.(DAGMAR et al., 2015) Synthesis of polymers in micro- or milli-reactors is drawing the scientific community's attention to access pathways inaccessible in conventional reactors. (MENDEZ-PORTILLO, 2011) Moreso, it is important to precisely tune the properties of the end-use polymer as well as other prevailing factors involved in the scalable synthesis of the polymer such as control for safety and quality assurance. (MASTAN and ZHU, 2015)

Mathematical modelling and simulation of chain growth polymerization reactions can be classified mainly as either stochastic or deterministic modelling approaches. Stochastic modelling functions on the premise of the laws of probability. More precisely, it models the differential form of the Chemical Master Equation (CME). Moreso, in the context of probabilistic laws, Markov chain theory is incorporated to provide insights into the correlations among factors such as overall kinetics of the polymerization reactions and ultimately the resulting polymer microstructure. Thus, this information can be used to optimize the polymerization reaction in order to tailor the polymer's

end-use properties. (HIDETAKA, 2015; Tobita, 1998) Hence, while the history of the chain growth reaction becomes irrelevant, the latest state of the chemical reaction system represents or produces an ensemble of stochastic trajectories that fully describe the chemical reaction system.

In contrast, deterministic modelling is more appropriate for Rate Reaction Equations (RRE). In the context of this work, taking population balances will give rise to up to 100,000 ODEs representing each reaction taking place within the chain growth polymerization reaction per macromolecule. Hence, approximate techniques like Method of Moment (MoM) are widely employed. There have been numerous applications of modified SSAs such as the Kinetic Monte Carlo (KMC) based on the Gillespie Algorithm (GA) to simulate FRP reactions with monofunctional initiators which were also used extensively as reported in the literature. (TOBITA, 1996)

Overall, the computational cost and efficiency in simulating polymerisation systems are key factors to be considered hence, the call for implementing a robust algorithm for modelling and simulation of such chemical reaction systems is very paramount. Thus, it is believed that a hybrid Gillespie algorithm could provide a more scalable and reliable technique to overcome the pre-existing challenges associated with stochastic modelling of chain growth polymerization reactions.

1.2 Objective

The main aim of the project is to find an effective, robust and scalable approach to simulating Free Radical Polymerization (FRP) of styrene in microchannels by mimicking a micro- or milli-reactor volume. Thus, the specific objectives are:

1 To investigate the statistical discrepancies between experimental and simulated results by taking into account the varying input conditions such as operating temperature, feed ratio of monomer to solvent as well as that of the initiator.

2 Efficiently compute the rate of monomer conversion as well as the molecular weight distribution of the polymer without employing the traditional statistical moments techniques which assumes the Long-Chain Approximation (LCA) or Quasi-Steady State Approximations (QSSA).

3 To apply a proposed hybrid stochastic simulation algorithm with the computing capability of initiating both stochastic and deterministic parallel simulations concurrently.

1.3 Structure of Thesis

Highlights of the thesis structure are as follows:

Chapter 2: **LITERATURE REVIEW**

1 Review of Free Radical Polymerization (FRP) as a form of the chain growth polymerization as well as its applications are discussed in this section.

2 An overview of polymerization reactions in microchannels are also discussed in this section.

Chapter 3: **STOCHASTIC MODELLING**

1 An introduction into Stochastic Simulation and Modelling techniques as well as its applications are treated in this section.

2 An introduction to the Chemical Master Equation (CME) is briefly highlighted with a supporting example.

3 A brief description of the Gillespie Algorithm (GA) is also summarized with brief mathematical derivations.

4 In addition, the Tau - Leaping technique is also reviewed in this section.

5 Finally, a classification tree of the Stochastic Simulation Algorithm (SSA) is introduced. Each branch of the SSA and their computational applications are discussed in details in this section.

Chapter 4: **METHODOLOGY AND APPLICATION OF THE HYBRID STOCHASTIC SIMULATION ALGORITHM (HSSA)**

1 The application of the hybrid stochastic simulation algorithm to the Free Radical Polymerization (FRP) of styrene monomer in microchannels is explored in this section.

2 The methodology or work-flow of this project is elaborated in this section.

3 The computation of the end-use properties of the polymer such as the rate monomer conversion rate, molecular weight distributions and polydispersity index using the Hybrid Stochastic Simulation Algorithm are discussed in this section.

Chapter 5: **RESULTS AND DISCUSSIONS**

1 Analysis of the obtained results from the Hybrid Stochastic Simulation Algorithm and discussions of the same are carried-out in this section .

2 Furthermore, a comparative analysis of the simulation versus experimental results is also discussed in this section.

Chapter 6: **Concluding Remarks and Future Outlook.**

1 Concluding remarks of simulated results.

2 Future Outlook.

CHAPTER 2
LITERATURE REVIEW

2.1 Overview of Free Radical Polymerization (FRP)

The wide use of polymers cannot be overemphasized and their production is estimated to exponentially increase from its current rate as sustainable polymer products are anticipated to replace metals in the automobile industry and other sectors. Some innovative examples of polymers finding increasing applications in the industry are Self-Healing Polymers (SHP) which have the ability to repair themselves when damaged, fractured or subjected to very high tensile stress. They find applications in paints and coatings, adhesives and in other composite materials. Graphene-Reinforced Polymers (GRP) which are composite materials with a combination of strength and conductivity. GRPs finds applications in the automotive, electronics and the energy industry. Another interesting example are the Biodegradable polymers (BP), they are formed from renewable sources such as sugarcane. BPs are replacing non-biodegradable or traditional plastics in packaging of consumer goods hence, offering environmental sustainable solutions. Other prominent polymers are Shape-Memory Polymers (SMP), Stimuli-Responsive Polymers (SRP) and Conductive Polymers (CP). (El-Ghoul et al., 2021; Rego et al., 2020)

The formation of polymers is produced via various methods of polymerization. They constitute several chains made up of repeated structural units or monomers. These polymeric chains can either be linear, branched, or cross-linked. Thus, it is worth noting that, these chain configurations reveal the type of polymer characteristics such as chemical and physical properties. Polymerization can be classified broadly as chain reaction (or addition) and step reaction (or condensation). While chain reaction polymerization requires the presence of an initiator to commence propagation via a radical (could be a free radical, cation or anion) transfer mechanism, the step reaction form of polymerization requires bi-functional or poly-functional monomers to propagate. (STUART et al., 2010)

By definition, Free Radical Polymerization (FRP) is a branch of chain polymerization through which polymers are formed by the successive addition of radical building molecular blocks or repeated units (activated monomer). This reaction comprises mainly the chain initiation, chain propagation, chain termination and possible chain transfers to monomer, solvent or another active component of the polymerization process. Moreso, FRP is applied widely in the synthesis of different polymers and material composites due to the versatility of the reaction. (WARD, 2009; ODIAN, 2004) Other common types of Radical polymerization (RP) employed in the industry are:

1 Bulk polymerization reaction: This polymerization involves the mixture of only an initiator (or co-initiator) and monomer, but no solvent. (WARD, 2009)

2 Solution polymerization reaction: Unlike Bulk Polymerization reaction, it contains a mixture of solvent, initiator, and monomer. (WARD, 2009)

3 Suspension polymerization reaction: This is a heterogeneous radical polymerization technique which uses mechanical mixing to mix a monomer or combination of monomers in a liquid phase, such as water. Furthermore, the monomer droplets are suspended in the liquid phase which are typically of size ranges of $10\mu m$ to $1000\mu m$. (WARD, 2009)

4 Emulsion polymerization: Unlike suspension polymerization, the initiator is soluble in the aqueous phase or media. An emulsifying agent such as polyoxyethylene alkyl ether is commonly used. (WARD, 2009; NAOYA, 2019)

Other forms of Radical Polymerization (RP) are Template Polymerization, Plasma Polymerization, Sonication, Atom Transfer Radical Polymerization (ATRP), Reversible Addition-Fragmentation Chain-Transfer Polymerization (RAFT), and Stable Free Radical Polymerization (SFRP). (ODIAN, 2004; WARD, 2009; DANIEL, 1997; KATO et al., 1995; XEROXCORP, 2003)

A typical FRP reaction pathway is illustrated by the chemistry of the reaction below:

Initiation:

$$I \xrightarrow{f,K_d} 2P^{\bullet}$$

Propagation:

$$P_n^{\bullet} + M \xrightarrow{K_P} P_{n+1}^{\bullet}$$

Termination (by Combination):

$$P_n^{\bullet} + P_m^{\bullet} \xrightarrow{K_{tc}} D_{n+m}$$

Termination (by Disproportionation):

$$P_n^{\bullet} + P_m^{\bullet} \xrightarrow{K_{td}} D_n + D_m$$

Chain Transfer to Monomer:

$$P_n^{\bullet} + M \xrightarrow{K_{trM}} P_1^{\bullet} + D_n$$

Chain Transfer to Solvent:

$$P_n^{\bullet} + S \xrightarrow{K_{trS}} P_1^{\bullet} + D_n$$

Where the parameters K_d, K_P, K_{tc}, K_{td}, K_{trM} and K_{trS} refer to the rate constant of initiator decomposition, monomer propagation, termination by combination, termination by disproportionation and chain transfer, respectively. Also I, M, $P^{\bullet}$, D represent the initiator, monomer, radical or live polymer, and dead polymer. Furthermore, f represents the initiator efficiency. The subscripts n and m in the above chemistry of reaction equations denote the number of monomeric units on the propagating or terminating chain. (MASTAN and ZHU, 2015)

In addition, aside from the efficiency of the initiator in FRP, another important factor that influence the degree of polymerization is the operating temperature. The higher the temperature, the higher the rate of chain propagation and thus, a higher degree of polymerization. The inverse is the case for the molecular weight at higher temperatures. Moreso, factors such as chain growth, chain transfer, chain termination and, the velocity constant of radical formation also play a role. (ODIAN, 2004; VIEIRA and LONA, 2016)

2.1.1 Free Radical Polymerization of styrene in the industry

Free radical polymerization is widely responsible for the synthesis of more than half of the polymers in the market. (MATYJASZEWSKI and GAYNOR, 2000) This is mainly hinged on the fact that FRP is not only cost-effective but also, an effective method for manufacturing high molecular weight polymers. Other choice reasons for the application of FRP in the industry are reduced manufacturing time, safety, insensitivity to impurities, and operation at moderately low temperatures. (MATYJASZEWSKI and GAYNOR, 2000; MOAD, 2016; HONG et al., 2002; VICEVIC, NOVAKOVIC, and BOODHOO, 2021)

Furthermore, while the focus of this research is centred on the industrial synthesis of polystyrene, it is worth mentioning that there are other polymers produced by free radical polymerization such as polypropylene (PP), high-density polyethylene (HDPE), linear low-density polyethylene (LLDPE), Low Density Polyethylene (LDPE), Polystyrene (PS) and Polyvinyl Chloride (PVC). Other smaller-volume polymers are polyesters, with poly(ethylene terephthalate) (PET), Engineering Plastics (EP), Acrylonitrile–Butadiene–Styrene (ABS) copolymers, polycarbonates (PCs), polyamides (PAs), polyurethanes (PURs), polysulfones (PSUs), polyetherketones (PEKs), polyetheretherketone (PEEKs), polyoxymethylene (POM), polyimides (PIs), polyphenylenesulfide (PPS), polyphenylene oxide (PPO), polytetrafluoroethylene

(PTFE) to mention a few. (MATYJASZEWSKI and GAYNOR, 2000)

Thus, this makes free radial polymerization of styrene a popular and versatile industrial process in the industry. Furthermore, FRP of styrene provides facile statistical copolymerization which limits loss by vaporization and thus, it is cost-effective. (NESVADBA, 2012; VICEVIC, NOVAKOVIC, and BOODHOO, 2021; SERRA, 2013) However, the following are shortcomings:

1. Formation of unwanted by-products, such as peroxides and hydroperoxides due to the non-specific nature of the free radicals.
2. Unwanted side reactions such as chain transfer.
3. Poor control of the reaction mechanism which leads to broader molecular weight distribution.

Overall, the commercial production of polystyrene has been widely achieved via the FRP of styrene monomer however, the lack of control over the polymer microstructure or architecture has resulted in researching ways to improve the process intensification. Hence, in the following subsection, the benefits of the FRP in microchannels (micro or milli reactor) will be highlighted. (BENOIT et al., 2000; IWUCHUKWU and VIANNA, 2023)

2.2 Polymerization reaction in microchannels

2.2.1 General overview of microchannels

Micro or milli reactors, otherwise termed microchannels, are gaining increasing application in various research fields. Microstructured or microchannel reactors are preferred for their energy-saving efficiency, scalability, reliability, yield, higher process control and improved yield. (FLAVIO et al., 2017; MILLS, J.Q, and JAMES, 2007) They are miniaturized chemical reactors that are suitable to operate at a microscale level. In other words, with a small surface area to volume ratio ranging from 100 to 10,000 m^2m^3, they provide high mixing rates, improved reaction control, short reaction times, enhanced heat and mass transfer coefficient as well as proven better choice for pilot experimentation over conventional reactors. (VOLKER, HOLGER, and FRIEDHELM, 2005)

Furthermore, microchannel reactors are primarily developed to improve chemical reaction conditions at a microscale (pilot scale) and then numbered up to improve

efficiency even at a larger or industrial scale. Moreso, due to their impact on reaction kinetics, they find application in the chemical, biological, engineering and nuclear energy fields to improve process or production efficiency as well as process safety. (MILLS, J.Q, and JAMES, 2007; TEUSCHEL, 2001; JÄHNISCH et al., 2004) However, a microreactor is quite expensive to set up when compared to traditional reactors.

Nonetheless, although the advantages of the usage far outweigh the disadvantages, it does not provide capital cost reduction when scaled and compared to conventional reactors. Hence, from an economy-of-scale standpoint, it still falls short of expectations. Moreover, aside from the common issues of clogging and fouling of the microreactor pores, there are also certain issues that need to be surmounted such as:

1 The need for certification and advanced design to carry out more complex research.

2 Being proven unsuitable for nuclear reaction research.

3 The relatively high cost when compared to traditional reactors.

Thus, due to the above shortcomings, this project is aimed at deploying the proposed stochastic simulation algorithm to better understand the challenges often caused by milli- or micro-reactors during polymerization reaction and thus proffer more accurate information for the process intensification of the FRP of styrene in microchannels. (KUMAR et al., 2022; JAISWAL et al., 2022; WILLE et al., 2004)

2.2.2 Previous studies on the stochastic simulation of the FRP of styrene

There have been previous research efforts channelled towards the application of stochastic simulation in the context of free radical polymerization. However, it is worth stating that while the investigation of the microstructure of the polymer formation has been investigated, there has not been so many investigation focused on the application of stochastic simulation in the context of polymer formation via microchannels or microreactor technology. (IWUCHUKWU and VIANNA, 2023)

Moreso, coupled with the shortcomings of the microreactor technology, one of the primary challenges associated with general polymerization reaction is the precise control and optimization of the reaction mechanism at a micro-scale. Hence, a stochastic simulation approach has been utilized to address the problems earlier highlighted when it comes to polymerization via microchannels. (YAO et al., 2015; SHUSAKU et al., 2017; SU, SONG, and XIANG, 2018) Thus, the review in this subsection is aimed to highlight a few closely aligned research efforts stating the importance of understanding

the polymer's microstructure in predicting its end-use property and enhancing the overall polymerization reaction. (IWUCHUKWU and VIANNA, 2023; CROMPTON, 1993; JÄHNISCH et al., 2004)

In his work, Soares (2004) reviewed various mathematical modelling techniques to quantify the microstructure of polymers. The review was aimed at emphasizing the importance of understanding the microstructural details and how they could impact the macroscopic properties of the polymer, especially by long chain formation and terminal branching. Moreso, the review was focused on the application of mathematical modelling methods such as the Method of Moment (MoM), Population balances, Instantaneous distribution and most importantly Monte Carlo simulation towards the modelling of the microstructure of polyolefins made by coordination polymerization. (J. SOARES, 2004)

Also, Shao, et al. (2015) also emphasized the importance of understanding the polymer formation at a microscale formed via FRP by deploying a hybrid Monte Carlo routine. The hybrid Monte Carlo routine used combines both reaction mechanisms of the FRP and a coarse-grained molecular simulation to study the chain growth reaction. However, the model represents the polymerization kinetics in both batch and semi-batch processes using the PRECIDI^{TM} software. Also, aside from obtaining promising monomer conversion and molecular weight distribution (MWD) results as the kinetic constant for chain propagation K_p was varied, the work did not account for the fast reaction dynamics comprising of chain initiation affected by the radical transfer. (SHAO et al., 2015)

Another similar work to the Hybrid Stochastic Simulation Algorithm (HSSA) used in this work was published by Amit and Donald (2015), which deployed a hybrid Monte Carlo simulation approach aimed at capturing both the fast and slow dynamics of a typical FRP reaction. The fast dynamics comprising radical transfer from the chain initiation step were simulated by stochastic simulation while, the chain propagation (slow dynamics) was accounted for by deterministic simulation. Although the results obtained were promising for a hypothetical case of a simple bulk FRP of Methyl Methacrylate (MMA) and also predicted viability for complex FRP reactions, the technique did not guarantee optimum application for small varying volume systems like a microchannel. (TRIPATHI and SUNDBERG, 2015; HSSA, 2022).

Stanislaw and Szymanski (2019) used a hybrid stochastic-deterministic technique in order to capture the fast dynamics of a controlled radical polymerization reaction. More specifically, the investigation involved the copolymerization of MMA with vinyl chloride as well as using hypothetical kinetic value reported in the work to test the hybrid Monte Carlo simulation method (HCBC) while comparing it to the GA. Interestingly,

the respective computing efficiencies of the GA and the HCBC were compared thus concluding that the GA was more robust in capturing the stochasticity of the FRP system at a microscale (or small volume). (STANISLAW and RYSZARD, 2019)

In the same vein, Gao et al. (2015) also proposed scaling techniques that entail scaling reaction rate or kinetic constants to accelerate the KMC simulations by a factor of 100. The proposed KMC used in the investigation proved to be effective for the FRP reaction mechanism with experimental or kinetic constants. While the work was projected to facilitate the linkage of the KMC output with standalone molecular simulations to understand the "structure-property" relationships such as chain sequence, polymer physical properties, glass transition temperature and mass transport properties, the "scaled-KMC" can only handle a limited volume of molecules, highlighting the limits of the scaling approach. (GAO and HE, 2015)

Most recently, Stanislaw and Szymanski (2022) confirmed that polymerization processes like the FRP could be carried-out in dispersed systems and have shown great potential for wide application. They further explained that based on the outcome of their investigation that this aspect is yet to be fully explored. Interestingly, their work was focused on understanding the impact of process conditions on the kinetics and end-use characteristics of a polymer via Living Polymerization at a nano-scale. Furthermore, they affirmed that chain growth polymerization in nano-channels (or droplets) would not be fully captured without deploying a stochastic technique to track droplets of low-number reacting species even at reacting large volumes. Moreso, by using a Normal or Poisson distribution to simulate the reactant molecules, taking place in nano-droplet dispersions fashion, a detailed description of both reversible and irreversible chain-growth polymerization processes can be understood. (SOSNOWSKI and SZYMANSKI, 2022)

Thus, it is worth re-emphasising that the choice for deploying a hybrid Gillespie Algorithm (GA) for the FRP of styrene in this work over a Kinetic Monte Carlo (KMC) framework is predicated on capturing the rates of slow and fast dynamics associated with the free radical transfer in the FRP of styrene. (IWUCHUKWU and VIANNA, 2023). Although the GA and KMC are powerful stochastic simulation methods for simulating the kinetics of complex chemical reactions and as well share similar computing frameworks in their algorithms, the following are the reasons for adopting the hybrid Gillespie algorithm over the Kinetic Monte Carlo technique (TRIGILIO et al., 2020) :

1 The GA is a function of the Chemical Master Equation (CME) which is unique to the type of chemical reaction in consideration, while the KMC adopts a Monte Carlo simulation framework to approximate the reaction kinetics regardless of the

type of reaction. Moreso, for a chain growth polymerization reaction, GA seems to be a good choice over KMC as it computes the individual reaction pathway propensities whereas, the KMC just predefines the individual rates of reaction pathways and then performs random sampling to determine the next reaction. (SLEPOY, THOMPSON, and PLIMPTON, 2008; D.T. GILLESPIE, 2007)

2 Unlike the GA which interprets the intrinsic stochastic behavior of the CME of chemical reaction systems, Monte Carlo simulations predominantly use random sampling which results in statistical error. The stochastic trajectories of the Monte Carlo simulations are subject to statistical variability. While the simulations provide estimates and probabilities, they are not precise predictions. Chain reaction steps like initiator decomposition and chain initiation of an FRP reaction may not be captured as they are latent reaction steps. (STAMATAKIS and D. VLACHOS, 2012)

3 Overall, the major limitation of the application of the KMC in chemical reactions is that the reaction rate has to be known in advance thus adopting a non-markovian process. In contrast, the GA works effectively in this scenario due to the fact it operates on the CME of the defined reaction system. Moreso, the KMC is effective for specific polymer reaction systems with structural configurations. (MAVRANTZAS, 2021)

Hence, if the FRP of styrene is to be carried-out in a microchannel (with a predefined volume), it is vital to consider an algorithm robust enough for smaller volume systems as well as a comparative low computational cost. Overall, this work aims to address the computational shortcomings of the above review by proposing an algorithm to efficiently predict the FRP of the styrene model and thus providing reliable information applicable for process intensification purpose.

CHAPTER 3
STOCHASTIC MODELLING

3.1 Stochastic Simulation and Modelling Techniques

Stochastic simulation of the kinetics of complex chemical systems like the FRP system has proven to be an effective technique for an in-depth understanding of a given chemical reaction system. (HAHL and KREMLING, 2016; MASTAN and ZHU, 2015; TIAN and BURRAGE, 2004; YANG CAO, D.T. GILLESPIE, and LINDA R. PETZOLD, 2006) As earlier stated, simulating the FRP system can be carried out by applying either deterministic or stochastic approaches. However, each simulation technique has its advantages and limitations, which influence their choice regarding the problem at hand. (MEIMAROGLOU and KIPARISSIDES, 2014; Y. CAO, D.T. GILLESPIE, and L. R. PETZOLD, 2005; SMITH, 2007)

To begin with, at low molecular copy numbers, the FRP system is inherently stiff to compute hence, a deterministic simulation approach is not robust to capture both the slow and fast dynamics of the system. (MASTAN and ZHU, 2015; MEIMAROGLOU and KIPARISSIDES, 2014) Secondly, the governing CMEs of the FRP system usually consist of a set of ODEs representing each reaction in the chain growth polymerization per macromolecule of the polymer, thus making it numerically intractable to solve deterministically. (MASON, HUDSON, and SUTTON, 2005; FICHTHORN and WEINBERG, 1991)

Notwithstanding, a deterministic approach is an available option when dealing with high molecular copy numbers. More specifically, solving the FRP numerically generates an infinitely large number of stiff ODEs. In turn, a statistical approach is employed to simulate the approximate properties of the polymer using methods of moments statistical techniques. (LAURENCE, GALVAN, and TIRRELL, 1994; SMITH, 2007) On the other hand, a stochastic approach seems to be more effective at low copy numbers.

Most recently, hybrid stochastic-deterministic methods are been developed to deal with the fast and slow dynamics of complex chemical reaction systems as well as considering the computational efficiency of the algorithm architecture. This slow and fast dynamics of a chemical reaction system are influenced by a number of factors which includes temperature variation for example. Moreover, the application of hybrid simulation algorithms brings a diversity of representations of the phenomenology of the chemical reaction in consideration. (BURKE, 2021) If certain factors surrounding the choice of the hybrid technique are sufficiently considered then, the choice could lead to interfacing complexity between models as well as scalability and computational efficiency. As described further in Chapter 4, a Hybrid Stochastic Simulation Algorithm (HSSA) is applied in the simulation of the FRP of styrene because of its capacity to perform parallel stochastic and deterministic simulations in order to capture both the fast and slow dynamics of the reaction and also, the robustness to simulates the chain growth up to $2^{31} - 1$ moles of the polymer.

3.2 The Chemical Master Equation (CME)

The Chemical Master Equation (CME) provides the fundamental basis for describing the rate of inter-molecular interactions. It forms the basis for modelling complex chemical reactions such as chain growth reactions as it is efficient in simulating stochastic noise produced from such reactions. In this context, these dynamical reaction systems are assumed to be well mixed and, at thermal equilibrium. The collisions between molecular species are also assumed to be random within the reaction volume and the momentum of head-on collisions of inter-molecular species is also assumed to be elastic.(D.T. GILLESPIE, 2007)

Furthermore, it has been a heavily applied tool for understanding discrete stochastic chemical reaction systems. Solving the CME model of complex systems is well-known to be intractable to solve. Hence, the Gillespie Algorithm proves to be an invaluable technique applied in solving the CME of a complex system. it is also worth noting that the Reaction Rate Equation (RRE) or Chemical Kinetic Equation (CKE) follows or obeys the law of mass action. Thus, the CME describes the inherent stochasticity with respect to reaction times resulting in varying copy numbers of the reacting species.

Consider a system with fixed volume, V at thermal equilibrium, T as well as a well-mixed chemical reaction system. Also, let the system constitute of molecular species $(S_1, S_2, S_3, \ldots, S_N)$ where $1 \leq i \leq N$ and the reaction pathways as $(R_1, R_2, R_3, \ldots, R_M)$ where $1 \leq j \leq M$. Again, after a reaction R_j occurs within an infinitesimal time dt, the updated molecular distribution of the respective species, S_i following the reaction R_j

is defined as a vector of coefficients $v_{ij} \in \mathbb{R}^N$ where $v_{ij} = (v_{1j}, v_{2j}, v_{3j}, \ldots, v_{Mj})$. Hence, the state vector v_{ij} (where i indexes the state variables, and j indexes the event(s)) containing the number of molecular species present in the system at a given time t. Another important variable is the propensity function, a_j which is the probability that a reaction R_j will occur within an infinitesimal time interval $(t, t + dt)$ in a reaction volume V given that it was initially in a state v_{ij} at time t. The inherent stochasticity of a chemical reaction system is described by the CME with the following summarized assumptions:

1 The system is well-mixed.

2 The CME follows a Markov process. This implies that the future state of the reaction depends solely on the current state and not on the history of the chemical reaction system.

3 The CME assumes a discrete state space. This implies that the consumption and formation of the reactant species are in discrete or integer numbers.

Let's assume a well-mixed chemical reaction system with species, S_i and reaction channels, R_j. Then, the current state of the system can be denoted as X. Also, the propensity $a_j(X)$ is the probability per unit time that reaction, R_j will occur given state, X.

In order to formulate the Chemical Master Equation (CME), one can consider the probability flux into and out of the state X. Then, the total probability flux out of state, X due to all reactions, R_j is given by:

$$\sum_{j=1}^{M} a_j(X)P(X,t) \tag{3.1}$$

Furthermore, the influx into state X comes from state $X - v_{ij}$ for all reaction, R_j that lead to state X:

$$\sum_{j=1}^{M} a_j(X - v_{ij})P(X - v_{ij}, t) \tag{3.2}$$

Hence, the total rate of change will be:
Probability flux into X - Probability flux out of X

Therefore:

$$\frac{\partial P(X,t)}{\partial t} = \sum_{j=1}^{M}\Big[a_j(X - v_{ij})P(X - v_{ij}, t) - a_j(X)P(X,t)\Big] \tag{3.3}$$

The above is the Chemical Master Equation (CME).

All in all, the Chemical Master Equation or CME provides a robust framework to model the stochasticity of the chemical reaction system by capturing the probabilistic nature of the molecular interactions. Thus, by solving the CME, the time-dependent probability distribution of the molecular population of a given system can be determined.

To further exemplify the CME, consider the set of chemical reactions consisting of two species from Figure 3.1:

$$A + 3B \xrightarrow{k_1} 2B$$
$$2B \xrightarrow{k_2} A$$

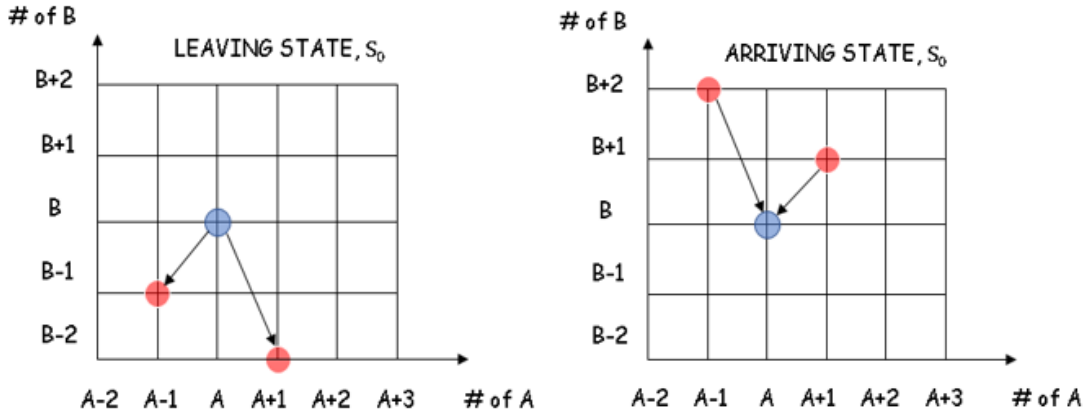

Figure 3.1: A 2-dimensional cartesian grid figure used for illustrating the formulation of the Chemical Master Equation (CME) for chemical reactions involving two species. The left grid plot shows two reactions taking place after an infinitesimal time dt from the original state, S_0 while, the right cartesian grid shows two different reactions arriving at the current state, S_0.

Furthermore, from the Figure (3.1), the two 2-dimensional cartesian grids with axes representing molar consumption or production of the interacting species namely A and B. The, left cartesian grid illustrates the two different reactions R_1, R_2 with states S_1, S_2 respectively taking place from the original state S_0 denoted by the blue circle in the figure above. The right cartesian grid illustrates the two reactions, R_1, R_2 with states S_1,

S_2 returning or arriving at the original state, S_0 then we have the following outcomes from the cartesian grid:

LEAVING STATE, S_0:

$S_{01} : (A, B) \rightarrow (A - 1, B - 1)$

$S_{02} : (A, B) \rightarrow (A + 1, B - 2)$

ARRIVING STATE, S_0:

$S_1 \rightarrow \mathrm{S}_0 : (A + 1, B + 1) \rightarrow (A, B)$

$S_2 \rightarrow \mathrm{S}_0 : (A - 1, B + 2) \rightarrow (A, B)$

To formulate the Chemical Master Equation (CME) for the given chemical reaction equation, consider the following possibilities:

1 For the first possibility, the probability for any reaction to arriving at a current state, S after an infinitesimal time, dt is $(A, B, t+dt)$ is either the state, S remained at (A, B, t) with no reaction taking place or at the current state, any of them had already taken place.

2 For the second possibility, the two reactions had already taken place.

Writing the CME, we have:

$$P(A, B, t+dt) = P(A, B, t)(1-k_1ABdt-k_2Bdt)+P(A+1, B+1, t)k_1(A+1)(B+1)dt + P(A-1, B+2, t)k_2(B+2)dt$$

$$P(A, B, t+dt)-P(A, B, t) = -(k_1AB-k_2B)P(A, B, t)dt+k_1(A+1)(B+1)P(A+1, B+1, t)dt + k_2(B+2)P(A-1, B+2, t)dt$$

Dividing both sides of the above equation by dt as $dt \rightarrow 0$ results to :

$$\frac{dP(A, B, t)}{dt} = -(k_1AB - k_2B)P(A, B, t) + k_1(A+1)(B+1)P(A+1, B+1, t)+ k_2(B+2)P(A-1, B+2, t)$$

3.3 Description of the Gillespie Algorithm (GA)

The Gillespie Algorithm (GA) or also known as the Stochastic Simulation Algorithm (SSA) was introduced to predict or simulate the exact realizations of biochemical or cellular reactions that involve interactions of millions of molecular species. It was first published in 1976 by Daniel.T Gillespie as an improvement on the Kinetic Monte Carlo (KMC) simulation technique, it has ever since been a fundamental approach for accounting for the inherent stochasticity in a complex chemical reaction which is latent when using traditional deterministic simulation methods. Although it is computationally expensive, it effectively solves the intractable nature of the CME that governs complex chemical reactions. (D.T. GILLESPIE, 2007)

3.3.1 Notation and Derivation of the Gillespie Algorithm (GA)

Once again, for M reactions $\{R_1, R_2, R_3, \ldots R_M\}$ where $1 \leq j \leq M$ and N molecular species $\{S_1, S_2, S_3, \ldots S_N\}$ for $1 \leq i \leq N$ while the state of the molecular species $\{X_1, X_2, X_3, \ldots X_N\}$ at time, t. Thus, to simulate the evolution of the system, the following question needs to be asked:

1 When will the next reaction occur?

2 Which reaction will occur next?

The answer to these questions will be $P(\tau, \mu)$. Where $P(\tau, \mu)$ is equal to the probability that given the state of the molecular species $\{X_1, X_2, X_3, \ldots X_N\}$ at a time, t:

1 The next reaction will occur in the infinitesimal time interval of $(t+\tau, t+\tau+d\tau)$ and,

2 The next reaction will be R_j.

It is worth noting that the time (τ) for the next reaction to occur is not necessarily infinitesimal. Then, applying the observations from the CME from the previous section, the probability that the next reaction, R_j will occur in the infinitesimal time interval $(t+\tau, t+\tau+d\tau)$ is $c_j h_j dt$. Where:
h_j = the number of instant combinations of reactants for reaction R_j.
c_j = propensity or stochastic constant. Thus, computing the probability that no reaction occurs in the time interval $(t, t+\tau)$ is given by:

$$P(\tau, j) = P_0(\tau)\, c_j h_j d\tau \tag{3.4}$$

Furthermore, given that $P_0(\tau)$, is the probability that no reaction occurs in the time interval $(t, t+\tau)$. Then, for an infinitesimal time interval of $d\tau$, no reaction can be assumed not to occur in the time interval$(t, t+\tau+d\tau)$ given the following:

1 No reaction occurs in $(t, t+\tau)$ and in the infinitesimal time interval of $t+\tau, t+\tau+d\tau$.

2 $(t, t+\tau)$ is very small but not always the case.

Applying the principles of the CME:

$$P_0(\tau+\delta\tau) = P_0(\tau)\left(1 - \sum_j c_j h_j d\tau\right) \tag{3.5}$$

Subtracting $P_0(\tau)$ from both sides of the above Equation (3.5):

$$P_0(\tau+\delta\tau) - P_0(\tau) = -P_0(\tau)\left(\sum_j c_j h_j d\tau\right) \tag{3.6}$$

The Equation (3.6) above becomes:

$$dP_0(\tau) = -P_0(\tau)\sum_j c_j h_j d\tau \tag{3.7}$$

Integrating the above Equation (3.7) as $\delta\tau \to 0$ then:

$$P_0(\tau) = e^{-\sum_j c_j h_j} \tag{3.8}$$

Finally, the above Equation (3.8) becomes:

$$P(\tau) = c_j h_j e^{-\alpha_j \tau} \tag{3.9}$$

For all $\tau \geq 0$ and $j = 1, 2, 3, \ldots, N$ where $\alpha_j = \sum_j c_j h_j$

Or by defining $X(t) = x$

$$P(\tau, j|x, t) = c_j h_j e^{-\alpha_j(x)\tau} \tag{3.10}$$

Furthermore, to compute τ, add natural logarithm to both sides of Equation (3.10):

$$\ln P(\tau, j|x, t) = \ln c_j h_j e^{-\alpha_j(x)\tau} \tag{3.11}$$

$$\ln P(\tau, j|x, t) = -\alpha_j(x)\tau \ln c_j h_j \tag{3.12}$$

$$\tau = \frac{1}{\alpha_j(x)} \ln \frac{c_j h_j}{P\left(\tau, j|x,t\right)} \tag{3.13}$$

Let $\xi_1 = \frac{P(\tau,j|x,t)}{c_j h_j}$ then:

$$\tau = \frac{1}{\alpha_j(x)} \ln \left(\frac{1}{\xi_1}\right) \tag{3.14}$$

Also, since the respective chemical reaction channel, R_j partitions the initially defined reaction time t then, the next reaction is determined by generating a second random number, ξ_2 from a Uniformly Random Distribution (URD) from the given time interval which satisfies the condition:

$$\xi_2 \geq \frac{1}{\alpha_0} \sum_{\mu=1}^{j-1} \alpha_\mu(x) \quad or \quad \xi_2 < \frac{1}{\alpha_0} \sum_{\mu=1}^{j} \alpha_\mu(x) \tag{3.15}$$

Re-writing the above Equation (3.15):

$$\frac{1}{\alpha_0} \sum_{\mu=1}^{j-1} \alpha_\mu(x) \leq \xi_2 < \frac{1}{\alpha_0} \sum_{\mu=1}^{j} \alpha_\mu(x) \tag{3.16}$$

Where α_0 is the cumulative sum of propensity after an iteration is completed and $\alpha_j(x)$ is the respective propensity for every reaction channel,R_j.

As shown in Equation (3.14), the value of τ is a function of the cumulative sum of propensities α of the successive chemical reactions taking place within the time interval, $d\tau$ and a variable ξ_1 which is obtained from a uniform distribution. Hence, the degree of discreteness of the simulation is dependent on the values of α and ξ. The original Gillespie Algorithm (Direct Method) is illustrated in the following steps below:

STEP 1 Initialize the simulation time, t and state change vector, v_{ij}. Where v_{ij} is the product of the molecular species and respective reaction channels, R_j.

STEP 2 Compute the cumulative sum of propensities of the respective reactions given by the equation below for every reaction channel, R_j where $j = (1, 2, 3, \ldots, N)$:

$$\alpha_j(x) = \sum_j c_j h_j$$

STEP 3 Generate two pseudorandom number ξ_1, ξ_2 from a Uniform Random Distribution (URD) or $\sim \mathcal{N}(0, 1)$. Again, compute the time for the next reaction $t \to t + \tau$ using Equation (3.14) :

$$\tau = \frac{1}{\alpha_j} \ln \left(\frac{1}{\xi_1}\right)$$

STEP 4 Compute the propensity of the next reaction , R_j using Equation (3.15) such that:

$$\frac{1}{\alpha_0}\sum_{j=1}^{M-1}\alpha_j(x) \leq \xi_2 < \frac{1}{\alpha_0}\sum_{j=1}^{M}\alpha_j(x)$$

STEP 5 Update the next reaction. The calculation stops until the number of iterations, n exceed the time of simulation, t_f where $n > t_f$.
Else:
Repeat **STEP 2**

3.4 The Tau-Leaping Technique

Also, put forward by Daniel T. Gillespie in 2001, the Tau-Leaping technique modifies the Gillespie Algorithm (GA) in the previous section. This technique sacrifices the exact simulation for an approximate simulation that is quicker to compute. As shown below in the following steps. The 'leaping condition' holds when there exists an infinitesimal time step $\tau > 0$ which is small enough to represent each reaction channel, R_j in the chemical reaction system. Furthermore, instead of computing the next infinitesimal time step for the next reaction, R_j, the algorithm 'leaps' forward in time following a Poisson Random Distribution (PRD) by updating the population of the respective molecular species in one step. (D.T. GILLESPIE, 2001)

Furthermore, the appropriate size of the 'leap' determines the accuracy of the algorithm thus, the larger the size of the 'leap', the higher the speed of implementation thus losing computational accuracy as a result. In contrast, a small 'leap' denotes many steps or iterations that may be captured for as many reaction channels R_j as possible hence, the algorithm would compute extremely slowly but with a higher degree of accuracy in terms of computation. Therefore, from each iteration, the propensity $\tau > 0$ will be a function of the leaping time τ and the number of occurrences k_j (or frequency of an event occurring within the defined 'leap') for every R_j sampled from a Poisson Random Distribution (PRD) is given by :

$$\lambda = P\left(k, \alpha_j(x)\tau\right) = \frac{e^{-\alpha_j(x)\tau}\left(\alpha_j(x)\tau\right)^k}{k!}\,(k = 0, 1, 2, \ldots) \tag{3.17}$$

Again, each iteration step of the Tau-Leaping algorithm is like an explicit Euler iteration technique :

$$X\left(t+\tau\right) = X\left(t\right) + \tau X^{'}(t) \tag{3.18}$$

Where $X^{'}$ is the updated state after iterating within the defined time frame $t \rightarrow t+\tau$ Thus, the state change for a reaction R_j is:

$$X\left(t+\tau\right)=X\left(t\right)+P_{j}\left(k,\alpha_{j}(x)\tau\right) \tag{3.19}$$

Overall, the approximate "leap" of the chemical reaction system within a time τ is given by:

$$X\left(t+\tau\right)=X\left(t\right)+\sum_{j=1}^{M}P_{j}(\alpha_{j}(x)\tau)v_{ij} \tag{3.20}$$

STEP 1 Initialize the simulation time, t and, the initial state of reacting species' $\{X_1, X_2, X_3, \ldots X_N\}$ state change vector, v_{ij}.

STEP 2 For every reaction channel R_j,where $j = 1, 2, 3, \ldots, N$, choose the time step , τ or the "Leaping Condition" such that $t \rightarrow t + \tau$

STEP 3 Compute the cummulative sum of propensities of the respective reactions for every reaction channel, R_j, where $j = 1, 2, 3, \ldots, N$:

$$\alpha_{j}(x)=\sum_{j}c_{j}h_{j}$$

STEP 4 For every reaction channel,R_j compute the number of occurrences, k_j Poisson(R_j) within the "Leaping Condition" given by Equation (3.17):

$$\lambda=\frac{e^{-\alpha_{j}\tau}\left(\alpha_{j}(x)\tau\right)^{k}}{k!}$$

Where $k = 0, 1, 2, \ldots, N$

STEP 5 Update the state of the respective molecular species:

$$X \rightarrow X + \lambda$$

And,

Compute the propensity of the next reaction , R_j using Equation (3.15) such that:

$$\frac{1}{\alpha_{0}}\sum_{j=1}^{j-1}\alpha_{j}(x)\leq\xi_{2}<\frac{1}{\alpha_{0}}\sum_{j=1}^{j}\alpha_{j}(x)$$

STEP 6 Stop calculation until the number of iterations, n exceeds the time of simulation, t_f where $n > t_f$. Else:

Repeat **STEP 2**

It is also worth noting that, the deterministic rate constants or kinetic rate constants are converted to stochastic rate constants based on the number of molecules of each reacting species present in the reaction volume within the predefined time of the simulation. According to Daniel T. Gillespie, the kinetic rate constants are transformed mathematically into stochastic rate constants with the following equations (D.T. GILLESPIE, 2007):

For unimolecular reactions.:

$$k^{Experimental} = k^{Stochastic} \tag{3.21}$$

For bimolecular reactions between different species.:

$$k^{Experimental} = \frac{k^{Stochastic}}{V.N_A} \tag{3.22}$$

For bimolecular reactions between same species.:

$$k^{Experimental} = \frac{2k^{Stochastic}}{V.N_A} \tag{3.23}$$

For termolecular reactions between same species.:

$$k^{Experimental} = \frac{6k^{Stochastic}}{V.N_A} \tag{3.24}$$

Where V is the reactor volume and N_A is the Avogadro number. For this work, the respective propensity functions of the reaction steps for the FRP of styrene are shown in Table (3.1) below.

Table 3.1: A table depicting the Free Radical Polymerization (FRP) steps and their respective propensity functions.

CHEMICAL REACTION	CHEMICAL REACTION EQUATION	REACTION RATE EQUATION, r_i	PROPENSITY FUNCTION, a_j
Initiator Decomposition	$I \xrightarrow{K_d} 2fR^\bullet$	$-r_I = 2fK_dI$	$a_I = k_I s_I$
Chemical Initiation	$R^\bullet + M \xrightarrow{K_i} R1^\bullet$	$-r_i = K_i M R^\bullet$	$a_i = k_i s_M s_{R^\bullet}$
Thermal Initiation	$3M \xrightarrow{K_{iterm}} R_1^\bullet + R_2^\bullet$	$-r_M = K_{iterm} M^3$	$a_M = \frac{1}{6} k_{iterm} s_M (s_M - 1)(s_M - 2)$
First Chain propagation	$R_1^\bullet + M \xrightarrow{4K_p} P_2^\bullet$	$-r_{M_1} = 4K_p M R_1^\bullet$	$a_{M_1} = k_P s_M s_{R_1^\bullet}$
Second Chain propagation	$R_2^\bullet + M \xrightarrow{4K_p} P_3^\bullet$	$-r_{M_2} = 4K_p M R_2^\bullet$	$a_{M_2} = k_P s_M s_{R_2^\bullet}$
Chain Propagation	$P_n^\bullet + M \xrightarrow{K_p} P_{n+1}^\bullet$	$-r_n = K_p M P_n^\bullet$	$a_n = k_p s_M s_{P_n^\bullet}$
Chain Transfer to Monomer	$P_n^\bullet + M \xrightarrow{K_{trM}} P_1^\bullet + D_n$	$-r_{trM} = K_{trM} M P_n^\bullet$	$a_{trM} = k_{trM} s_M s_{Pn^\bullet}$
Chain Transfer to Solvent	$P_n^\bullet + S \xrightarrow{K_{trS}} P_1^\bullet + D_n$	$-r_{trS} = K_{trS} S P_n^\bullet$	$a_{trS} = k_{trS} s_S s_{Pn^\bullet}$
Chain Termination By Recombination	$P_n^\bullet + P_m^\bullet \xrightarrow{K_{tc}} D_{n+m}$	$-r_{tc} = K_{tc} P_n^\bullet P_m^\bullet$	$a_{tc} = k_{tc} s_{Pn^\bullet} s_{Pm^\bullet}$
Chain Termination By Disproportionation	$P_n^\bullet + P_m^\bullet \xrightarrow{K_{td}} D_n + D_m$	$-r_{td} = K_{td} P_n^\bullet P_m^\bullet$	$a_{td} = k_{td} s_{Pn^\bullet} s_{Pm^\bullet}$

3.5 Classification of the Stochastic Simulation Algorithm

There are some other variants of the Gillespie Algorithm (GA) or Stochastic Simulation Algorithm (SSA) as shown in the classification tree of the SSA in Figure (3.2). (D.T. GILLESPIE, 2007) They offer not only computational speed to the intractable nature of the CME of complex chemical systems such as chain growth polymerization but also, robust enough to minimize errors due to approximation from these variants. A number of these variants or algorithms are reformulations for various cases of chemical reactions such as hybrid models, involving both continuous and discrete variability. There has been a quest to provide computational modifications of the GA for chemical reactions such as the FRP in order to increase the efficiency of the algorithm in terms of simulation time and speed. (D.T. GILLESPIE, 2001; TIAN and BURRAGE, 2004; Y. CAO, D.T. GILLESPIE, and L. R. PETZOLD, 2005; YANG CAO, D.T. GILLESPIE, and LINDA R. PETZOLD, 2006)

Below are highlights of the simulation technique depicted in the classification tree in Figure 3.2.

3.5.1 EXACT METHODS

3.5.1.1 Direct Method (DM)

The Direct Method for SSA forms the foundation of the Gillespie Algorithm (GA) and is fully explained in subsection 3.3.1.

3.5.1.2 Rejection-Based Method (RBM)

Here, this thesis is only intended to give a brief highlight of the algorithm hence, further proof of the Rejection-Based method explanation can be found in the publication by Thanh et al. (2014). The algorithm follows the given steps below (THANH, PRIAMI, and ZUNINO, 2014):

1 Compute upper and lower bound propensities, $\bar{\alpha}_j$, $\underline{\alpha}_j$ for $j = 1, 2, 3, \ldots, M$ for the next reaction, R_j. This is used to maximize or minimize the propensity function, α_j over the fluctuation interval of the respective states at a given time $\bar{X}, \underline{X}$. Thus, $\underline{X} < X(t) < \bar{X}$ holds for each species and also, the invariant $\underline{\alpha}_j \leq \alpha_j \leq \bar{\alpha}_j$ also holds for each reaction channel, R_j for $j = 1, 2, 3, \ldots, M$.

2 Generate ξ_1, ξ_2, ξ_3 for a $\sim \mathcal{N}(0, 1)$ and compute the next reaction, R_μ . Given that:

$$\frac{\bar{\alpha}_\mu}{\bar{\alpha}_0} \; and \; \bar{\alpha}_0 = \sum_{j=1}^{M} \bar{\alpha}_j$$

The next reaction, R_μ is selected when the condition is satisfied:

$$\sum_{j=1}^{M} \bar{\alpha}_j > \xi_1 . \bar{\alpha}_0 \tag{3.25}$$

3 Using the rejection-based test, the acceptance and rejection of the next reaction, R_μ is identified using the mathematical relation:

$$\xi_2 \leq \frac{\alpha_\mu}{\bar{\alpha}_\mu} < \frac{\alpha_\mu}{\bar{\alpha}_\mu} \tag{3.26}$$

If satisfied, adopt, R_μ. Otherwise, re-compute, α_μ

4 Compute the corresponding value of τ for the accepted R_μ following an Erlang distribution. Hence, for every k trials of the accepted R_μ (or $k - i$ rejected candidates), the firing time τ is given by:

$$\tau = \sum_{i=1}^{k} \frac{-1}{\bar{\alpha}_0} \ln u_i = \frac{-1}{\bar{\alpha}_0} \ln(\prod_{i=1}^{k} u_i) \tag{3.27}$$

Where $u = u.\xi_3$ is set for every successive iteration. The loop stops until $X \in [\underline{X}, \bar{X}]$ is fulfilled.

Overall, with the time complexity of $O(N)$, experiments have shown that the Rejection-based method (RBM) is roughly 20% faster than the Direct Method (DM), and the Next reaction method (NRM). It is worth noting that the N is the number of iterations required to compute the time τ required. However, the algorithm computes all possible reaction channels at each time step as well as the rejected non-occurring reaction. This mechanism, therefore, can prove not only to be time-consuming but, also to occupy a lot of memory space. (GAO and HE, 2015; DUAN and LIU, 2015)

3.5.1.3 First-Reaction Method (FRM)

As another classification of the exact method, it differs from the DM in terms of how the next reaction, R_j is selected. Moreso, the FRM selects the reaction, R_j with the least firing time to take place. Thus, in addition to **STEP 3** in the GA or DM, the following is implemented to determine the next reaction time τ:

$$\tau = \min(\tau_1, \tau_2, \tau_3, \ldots, \tau_M)$$

Where j is the index of $\min(\tau_1, \tau_2, \tau_3, \ldots, \tau_M)$. The algorithm has a time complexity of $0(M)$ where M is the number of selected reactions to occur next at a given state. Although the FRM is an improvement over the DM, its shortcomings are evident when the reaction system consists of reaction channels with similar propensities. (D.T. GILLESPIE, 1977)

3.5.1.3.1 Next reaction Method (NRM)

Another modified version of the DM was introduced by Gibson, M. and Bruck, J. in 2000. It is called the Next Reaction Method (NRM). One of the key features of the NRM is that the $(M-1)$ unused reaction times, τ are re-used during the simulation. In addition, the generated random numbers ξ_1, ξ_2 in **STEP 2** are computed more effectively using a dependency graph or an indexed priority queue. Thus, due to this robust feature of the NRM, it has a time complexity of $0(\log M)$. Where M is the number of selected reactions. (GIBSON and BRUCK, 2000)

In contrast to the advanced and robust features of the NRM over the DM, its shortcoming is predicated on the fact that the time of computation tends to increase when the chemical reaction system contains similar propensities for every reaction channel, R_j thus, increase the cost of computation due the use large sorted data structures. (GIBSON and BRUCK, 2000)

3.5.2 TAU-LEAPING METHODS

The Tau-Leaping or τ-Leaping method is a technique to accelerate the SSA while sacrificing the accuracy of the algorithm. As earlier highlighted in the previous subsection of this chapter, the effectiveness of the algorithm relies mainly on the "leap" or τ as its amount also affects the propensity, α_j of every reaction channel, R_j fired. Below are brief highlights of the other variants of the Tau-leaping algorithm. (D.T. GILLESPIE, 2001; D.T. GILLESPIE, 2007)

3.5.2.1 Explicit Tau-Leaping Method

As earlier explained in section (3.5), the explicit tau-leaping technique is a variant of the Tau-Leaping method. According to Equation (3.20), it follows the explicit Euler iteration technique. It is worth noting that the aim of the method is to reduce the computational cost compared to the Direct SSA while introducing the Poisson distributed approximation of each reaction channel R_j fired. Again, while the Poisson-generated random number K_j may seem to make the reactant species population negative, the main challenge with the unboundedness of the Poisson-generated numbers K_j is the lack of coordination of the tau-leaping technique deployed between each reaction channel R_j fired. Nevertheless, there have been computational improvements to rectify the problem. (D.T. GILLESPIE, 2001; Y. CAO, D.T. GILLESPIE, and L. R. PETZOLD, 2005; CHATTERJEE, D. G. VLACHOS, and KATSOULAKIS, 2005; TIAN and BURRAGE, 2004)

3.5.2.2 Implicit Tau-Leaping Method

The implicit τ-leaping technique is another variant of the Tau-Leaping that is also employed to increase the computational speed as well as minimize error upon computation. Like the Explicit Tau-Leaping, the algorithm also deploys the implicit Euler iteration technique. However, as the value of the "leap" increases to larger values, the computational efforts outweigh the accuracy it brings. (D.T. GILLESPIE, 2007)

Furthermore, in the context of applying the implicit Euler iteration model to the τ-leaping algorithm contradicts the Markov process theory. Nonetheless, Rathinam et al.(2003) proposed the following equation to correct the doubt observed earlier. (RATHINAM et al., 2003)

$$X\left(t+\tau\right)=X\left(t\right)+\sum_{j=1}^{M}P_{j}[(K_{j}(\alpha_{j}(x)\tau)-\alpha_{j}(x)\tau+\alpha_{j}(X(t+\tau))\tau]v_{ij} \tag{3.28}$$

The above Equation 3.28 is applicable to stiff ODEs and some tests have shown that its computational speed outweighs the Explicit τ-Leaping technique. Also, an important advantage of this technique is that for every Poisson random generated number (K_j), the resulting equation can be solved by deterministic techniques such as implicit ODE solvers. (ASCHER and LINDA, 1998)

3.5.2.3 Slow-Scale Tau-Leaping Method

The slow-scale Tau-leaping algorithm is also a variant of the Tau-leaping technique proposed by Yang and Petzold (2008) to handle multiscale stochastic simulation by combining the power of the slow-scale Stochastic Simulation Algorithm and adaptive tau-leaping method to understand complex reversible reaction systems. This work is not intended to extensively explain the slow-scale Tau-leaping methods as further information can be found in the work earlier referenced. (Y. CAO and L. PETZOLD, 2008)

In brief, a highlight of the low-scale Stochastic Simulation Algorithm and adaptive tau-leaping method are discussed here. The adaptive tau-leaping method is a technique introduced to effectively select the maximum value of τ in order to choose the optimal or best "leap" for the τ-leaping algorithm. Cao et al. (2006) proposed the equation below (YANG CAO, D.T. GILLESPIE, and LINDA R. PETZOLD, 2006):

$$\tau=\min_{i\in I_{rs}}\left\{\frac{\max\left\{\frac{\epsilon\chi_{i}}{g_{i}},1\right\}}{\left|\mu_{i}\left(\chi\right)\right|},\frac{\max\left\{\frac{\epsilon\chi_{i}}{g_{i}},1\right\}^{2}}{\sigma_{i}^{2}\left(\chi\right)}\right\} \tag{3.29}$$

Where I_{rs} = is the set of indices of all reactants. And, g_i = is the higher order of reaction (HOR) in which the reacting species, S_i occurs.

Whereby, for example, if :
$g_i = 1$ then, HOR (i) = 1.

Also;

If $g_i = 2$ then, HOR (2) = 2.

Or else, the reaction involved results in the consumption of two (2) molecular species, then:

$$g_i = \left(2 + \frac{1}{\chi_i - 1}\right) \tag{3.30}$$

Also, the mean μ and standard deviation σ^2 are given by:

$$\mu_i(\chi) \triangleq \sum_{j \in J_{ncr}} v_{ij}\alpha_j(\chi) \tag{3.31}$$

$$\sigma_i^2(\chi) \triangleq \sum_{j \in J_{ncr}} v_{ij}^2\alpha_j(\chi) \tag{3.32}$$

On the other hand, the slow-scale SSA was inspired by the intractable nature of the ODEs derived from the Michaelis-Menten enzymatic equation. The algorithm developed by Cao et al. (2005) primarily involves the following steps (Y. CAO, D.T GILLESPIE, and L. PETZOLD, 2005) :

1. Partition the reaction channels $R = R_1, R_2, R_3, \ldots, R_M$ into fast and slow subsets namely R^f and R^s respectively. Reaction channels whose propensity functions are large are assigned to R^f the remaining to R^s.

2. Split the species $S = S_1, S_2, S_3, \ldots, S_N$ into fast and slow subsets, S^f and S^s. Moreso, the rule of assignment is that any specie whose population get changed by a fast reaction channel, R^f is classified as a fast specie, S^f while others are categorized as slow, S^s. However, it is worth noting that a fast species, S^f can be changed by slow reactions, R^s but, a slow species, S^s cannot be changed or transformed by a fast reaction, R^f.

3. Define a virtual fast reaction, $\hat{X}^f(t)$ as the fast species population evolving only under the fast reaction, R^f i.e., $\hat{X}^f(t)$ is $X^f(t)$ with all the slow reactions, R_M^s switched off. Moreso, it with noting that while $\hat{X}^f(t)$ is a Markov process, $X^f(t)$ is a non-Markovian process.

4. Establish the following stochastic stiffness conditions:

   4.1. $\hat{X^f}(t)$ must be stable as it approaches $t \to \infty$ in well-defined time-independent random variable $\hat{X^f}(\infty)$.

   4.2. Next, ensure the limit $\hat{X^f}(t) \to \hat{X^f}(\infty)$ must be effectively accomplished in a time frame that is small compared with the expected time to the next slow reaction, R^s.

5. Finally, after the stochastic stiffness condition has been met, the $ssSSA$ is invoked by following the slow scale approximation which states the fast reaction, R^f can be ignored thus simulating the chemical reaction system one slow reaction, R^s at a time provided the propensity function for each slow reaction, R^s is replaced by its average with respect to the asymptotic virtual fast process, $\hat{X^f}(\infty)$. That is if $\hat{P}(y^f, \infty|X^f, X^s)$ is the probability that $\hat{X}(\infty) = y^f$ given that $X(t) = (X^f, X^s)$, then the propensity function $a_j^s(X^f, X^s)$ of each slow reaction R_j^s, at time, t can be approximated on the timescale of the slow reactions, R_j^s, by:

$$\bar{\alpha}_j^s = \sum_{y^f} \hat{P}(y^f, \infty|X^f, X^s)\alpha_j^s(y^f, X^s) \tag{3.33}$$

There have been recent further improvements of the slow scale tau-leaping method to solve slow and fast scale reactions which is common with stiff systems. Reshniak et al.(2019), proposed an improved algorithm termed " The Slow-scale split-step tau-leap method" by using time discretization exceeding the scale of the previous slow-scale tau-leaping algorithm. (RESHNIAK, KHALIQ, and VOSS, 2019)

3.5.3 APPROXIMATE METHODS

3.5.3.1 Chemical Langevin Method (CLM)

The Chemical Langevin Method is the application of stochastic simulation to model chemical reactions. The stochastic model referred to as the Chemical Langevin Equation (CLE) is a Stochastic Differential Equation (SDE) with a zero-mean Gaussian noise that describes the time evolution of the probability distribution of a chemical reaction system. Furthermore, as a coarse-grained model or discrete stochastic model, each reacting species represents an SDE thus, the solution of the jth stochastic equation at a given time t is a random variable representing the amount of j species within the same time frame. Again, it is worth noting that the CLE can be derived from the SSA through the τ-leaping method by the following assumptions as the system progresses from $\tau \to \tau + t$:

1 For every reaction channel R_j fired, the products $\alpha_j(x)\tau$ tends to be very large.

2 The leap time τ is negligibly small.

3 For every reaction channel R_j fired, each propensity function $\alpha_j(x)$ undergoes a relatively small change. Thus, $\alpha_j(x)\tau \gg 1$ for all $1 \leq j \leq M$.

Again, it is worth recalling that a Poisson random variable with a large mean is approximately equal to a normal random variable with the same mean and variance ($\mathcal{N}_j(\mu, \sigma^2)$). Hence, for every reaction channel R_j fired, the variable $\mathcal{N}_j(0,1)$ is a statistically independent normal random variable with mean 0 and variance 1. Then, Equation (3.20) becomes;

$$X(t+\tau) = X(t) + \sum_{j=1}^{M} P_j(\alpha_j(x)\tau, \alpha_j(x)\tau)v_{ij}Z_j \tag{3.34}$$

Where the Z_j is the independent normal $\mathcal{N}(0,\ 1)$ random variable defined earlier. Recalling the statistical identity, $\mathcal{N}(\mu,\ \sigma^2) = \mu + \sigma\mathcal{N}(0,1)$. Equation (3.34) becomes:

$$X(t+\tau) = X(t) + \sum_{j=1}^{M} P_j[(\alpha_j(x)\tau) + \sqrt{\alpha_j(x)\tau}Z_j]v_{ij} \tag{3.35}$$

Further expanding the Equation (3.35):

$$X(t+\tau) = X(t) + \sum_{j=1}^{M} P_j(v_{ij}\alpha_j(x)\tau) + \sum_{j=1}^{M} P_j(v_{ij}\sqrt{\alpha_j(x)}Z_j\sqrt{\tau}) \tag{3.36}$$

The above Equation (3.36) can be further rewritten by applying the theory of continuous Markov Processes:

$$\frac{dX(t)}{dt} = \sum_{j=1}^{M} P_j(v_{ij}\alpha_j X(t)) + \sum_{j=1}^{M} P_j(v_{ij}\sqrt{\alpha_j X(t)}dW_j(t) \tag{3.37}$$

The above Equation is called the Chemical Langevin Equation (CLE). $W_j(t)$ are independent scalar Brownian motions. Moreso, the above derived Equation (3.35) and (3.36) above also follow or obey the Chemical Fokker-Planck equation (CFPE). (D.T. GILLESPIE, 2007; HIGHAM, 2008)

3.5.3.1.1 Deterministic Simulation Method (DSM)

The Chemical Langevin Equation (CLE) further approximates the Deterministic Simulation Method as a chemical reaction system approaches its "Thermodynamic Limit" or macroscopic limit. (D.T. GILLESPIE, 2007) That is:

$$X_i, V \to \infty \ and \ X_i/V = Constant$$

Thus, as a system attains its macroscopic limit, every term in Equation (3.38) increases except for the stochastic part or the second part of the right-hand side of the

equation for the CLE thus approximating the deterministic simulation method. Hence, Equation (3.38) becomes :

$$\frac{dX(t)}{dt} = \sum_{j=1}^{M} P_j(v_{ij}\alpha_j X(t)) \tag{3.38}$$

3.5.4 HYBRID STOCHASTIC SIMULATION ALGORITHM (HSSA)

First introduced by Haseltine and Rawlings (2002), it is a subset of the Stochastic Simulation Algorithms, this technique integrates the functionalities of two or more variants depicted in the classification tree in the Figure (3.2) to increase the speed of computation, as well as robustness to solve the “stiffness” in complex chemical reactions. In this work, the HSSA employed is primarily applied to capture both the slow and fast dynamics of the FRP reaction. The fundamental application of the HSSA is explained further in section 4. (HASELTINE and RAWLINGS, 2002)

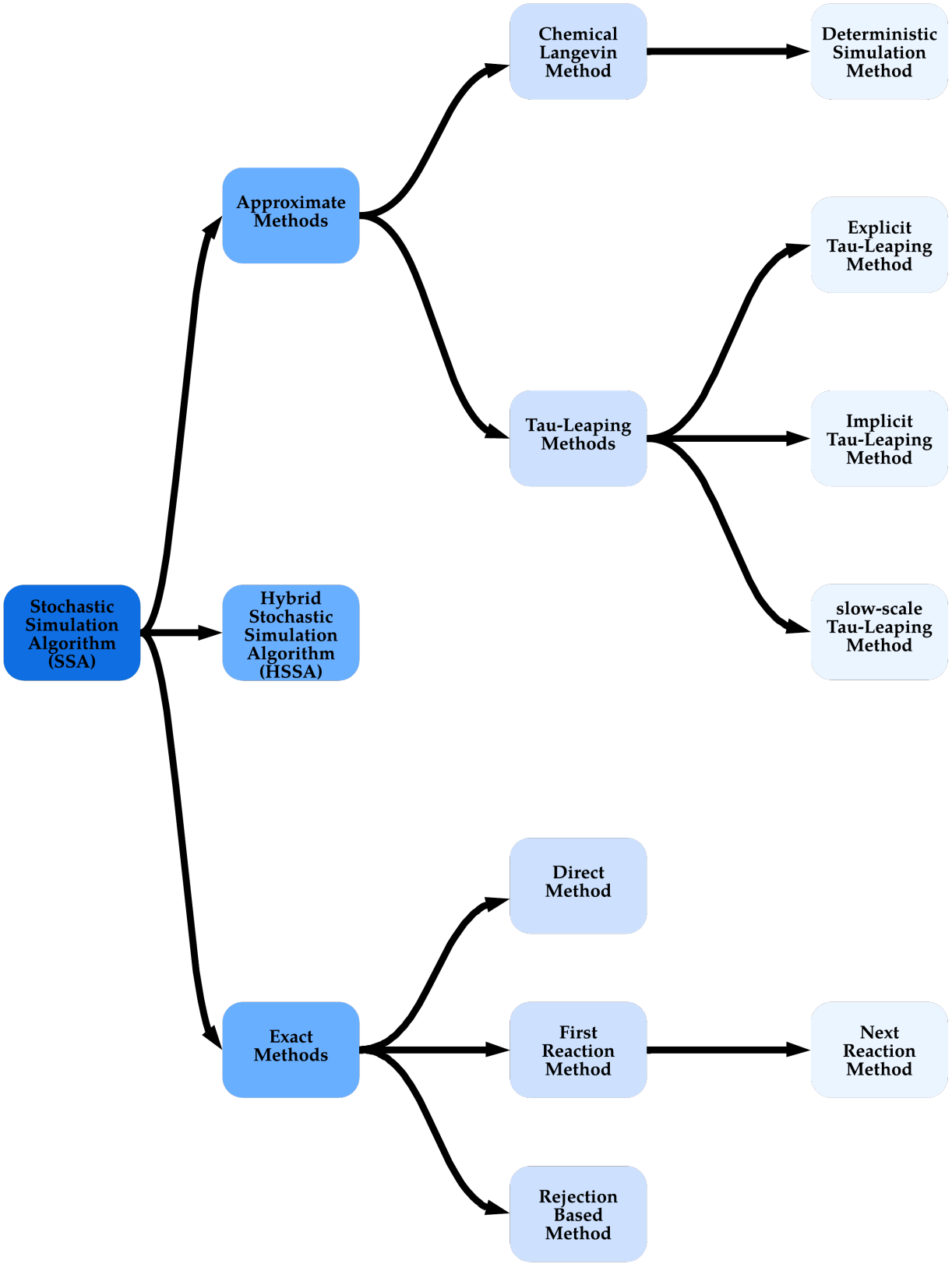

Figure 3.2: A schematic tree classification of the Gillespie Algorithm or the Stochastic Simulation Algorithm (SSA). Adapted from (D.T. GILLESPIE, 2007)

CHAPTER 4
METHODOLOGY AND APPLICATION OF THE HYBRID STOCHASTIC SIMULATION ALGORITHM (HSSA)

4.1 FRP of Styrene in microchannels

In general, Free Radical Polymerization (FRP) is one of the most effective techniques in synthesizing more than half the production of polymers worldwide. As earlier stated in Chapter 2, it is a chain polymerization method mainly made up of initiation, propagation, chain transfer, and termination steps. (CHIEFARI et al., 1998; SEYEDI et al., 2020; FU, CUNNINGHAM, and ROBIN A. HUTCHINSON, 2007) A phenomenological model for Free Radical Polymerization (FRP) of Styrene applied in this research is shown in the Table (4.1) below:

Table 4.1: A table showing each of the chain propagation steps of the FRP of styrene.

CHEMISTRY OF CHAIN REACTIONS	
$I \xrightarrow{K_d} 2fR^{\bullet}$ (4.1)	$P_n^{\bullet} + M \xrightarrow{K_P} P_{n+1}^{\bullet}$ (4.3)
$R^{\bullet} + M \xrightarrow{K_i} R_1^{\bullet}$ (4.1)	$P_n^{\bullet} + M \xrightarrow{K_{trM}} P_1^{\bullet} + D_n$ (4.4)
$3M \xrightarrow{K_{iterm}} M_1^{\bullet} + M_2^{\bullet}$ (4.2)	$P_n^{\bullet} + S \xrightarrow{K_{trS}} P_1^{\bullet} + D_n$ (4.5)
$M_1^{\bullet} + M \xrightarrow{4K_P} P_2^{\bullet}$ (4.2)	$P_n^{\bullet} + P_m^{\bullet} \xrightarrow{K_{tc}} D_{n+m}$ (4.6)
$M_2^{\bullet} + M \xrightarrow{4K_P} P_3^{\bullet}$ (4.2)	$P_n^{\bullet} + P_m^{\bullet} \xrightarrow{K_{td}} D_n + D_m$ (4.7)

Annotations:

(4.1): *Chemical Initiation Reaction*
(4.2): *Chain Transfer to Solvent Reaction*
(4.3): *Chain Termination by Combination Reaction*
(4.4): *Thermal Initiation Reaction*
(4.5): *Chain Propagation Reaction*
(4.6): *Chain Transfer to Monomer Reaction*
(4.7): *Chain Termination by Disproportionation Reaction.*

In this work, is it assumed that the chain termination is predominantly by dissociation thus the kinetic constant of termination by combination and dissociation are related as follows:

$$k_{tc} = 0 * k_t \qquad \& \qquad k_{td} = 1 * k_t \tag{4.8}$$

Where the initiator, solvent, monomer, live and dead polymer are denoted by I, S, M, P, and D respectively. Also, the respective kinetic constant for initiator dissociation, chemical initiation, thermal initiation, propagation, transfer to monomer, transfer to solvent, and termination by combination and disproportionation are K_d, K_i, K_{iterm}, K_p, K_{trM}, K_{trS}, K_{tc} and, K_{td}. The constant f at the chemical initiation step is referred to as the initiator's efficiency which ranges between $0.2 < f \leq 0.7$.

Assuming that a polymerization reactors is modelled as a microchannel thus, applying the conservation law of mass:

$$\frac{1}{V}\frac{d(Vc_j)}{dt} = R_j \tag{4.9}$$

Where:

V = reactor volume in cubic meters, m^3
t = simulation time in seconds, s
c_j = concentration of reacting species in $mol.dm^{-3}$
R_j = denotes the reaction between molecular species or reaction channels.

By applying Equation (4.9) above to the chemistry of reaction in Table (4.1), the following equations are obtained:

$$\frac{1}{V}\frac{d(IV)}{dt} = -K_d I$$

Since, the reactor volume V is constant then:

$$\frac{d(I)}{dt} = -K_d I \tag{4.10}$$

$$\frac{1}{V}\frac{d(MV)}{dt} = -K_i M R^\bullet - 3K_{iterm}M^3 - 4K_p M M_1^\bullet - 4K_p M M_2^\bullet \\ - K_p M \sum_{n-1}^{\infty} P_n^\bullet - K_{trM} M \sum_{n=1}^{\infty} P_n^\bullet - K_{trS} M \sum_{n=1}^{\infty} P_n^\bullet$$

$$\frac{d(M)}{dt} = -K_i M R^\bullet - 3K_{iterm}M^3 - 4K_p M M_1^\bullet - 4K_p M M_2^\bullet \\ - K_p M \sum_{n-1}^{\infty} P_n^\bullet - K_{trM} M \sum_{n=1}^{\infty} P_n^\bullet - K_{trS} M \sum_{n=1}^{\infty} P_n^\bullet \quad (4.11)$$

Let $M_1^\bullet \equiv M_2^\bullet \equiv R^\bullet$, the above Equation (4.11) :

$$\frac{d(M)}{dt} = -K_i M R^\bullet - 3K_{iterm}M^3 - 8K_p M R^\bullet \\ - K_p M \sum_{n-1}^{\infty} P_n^\bullet - K_{trM} M \sum_{n=1}^{\infty} P_n^\bullet - K_{trS} M \sum_{n=1}^{\infty} P_n^\bullet \quad (4.12)$$

Also from Table (4.1);

$$\frac{1}{V}\frac{d(R^\bullet V)}{dt} = 2fK_d I - 3K_i R^\bullet M b - 8K_p M R^\bullet$$

$$\frac{d(R^\bullet V)}{dt} = 2fK_d I - 3K_i R^\bullet M - 8K_p M R^\bullet \quad (4.13)$$

For live polymers:

$$\frac{1}{V}\frac{d(P_1^\bullet V)}{dt} = K_i R^\bullet M + K_{iterm}M^3 - 4K_p M R^\bullet \\ + K_{trM} M \sum_{n=1}^{\infty} P_n^\bullet + K_{trS} M \sum_{n=1}^{\infty} P_n^\bullet - K_{tc} P_1^\bullet \sum_{n-1}^{\infty} P_n^\bullet$$

$$\frac{d(P_1^\bullet)}{dt} = K_i R^\bullet M + K_{iterm} M^3 - 4K_p M R^\bullet + K_{trM} M \sum_{n=1}^{\infty} P_n^\bullet + K_{trS} M \sum_{n=1}^{\infty} P_n^\bullet - K_{tc} P_1^\bullet \sum_{n-1}^{\infty} P_n^\bullet \quad (4.14)$$

$$\frac{1}{V}\frac{d(P_2^\bullet V)}{dt} = K_{iterm} M^3 - 4K_p M R^\bullet - K_p M P_2^\bullet + K_p M P_1^\bullet - K_{trM} M P_2^\bullet - K_{trS} M P_2^\bullet - K_{tc} P_2^\bullet \sum_{n-1}^{\infty} P_n^\bullet$$

$$\frac{d(P_2^\bullet)}{dt} = K_{iterm} M^3 - 4K_p M R^\bullet - K_p M P_2^\bullet + K_p M P_1^\bullet - K_{trM} M P_2^\bullet - K_{trS} M P_2^\bullet - K_{tc} P_2^\bullet \sum_{n-1}^{\infty} P_n^\bullet \quad (4.15)$$

From Equation (4.14) and Equation (4.15) above:

$$\frac{1}{V}\frac{d(P_n^\bullet V)}{dt} = K_p M P_{n-1}^\bullet - K_p M P_n^\bullet - K_{trM} M P_n^\bullet - K_{trS} M P_n^\bullet - K_{tc} P_n^\bullet \sum_{n-1}^{\infty} P_n^\bullet, \quad n \gg 1.$$

$$\frac{d(P_n^\bullet)}{dt} = K_p M P_{n-1}^\bullet - K_p M P_n^\bullet - K_{trM} M P_n^\bullet - K_{trS} M P_n^\bullet - K_{tc} P_n^\bullet \sum_{n-1}^{\infty} P_n^\bullet, \quad n \gg 1. \quad (4.16)$$

Similarly for dead polymer:

$$\frac{1}{V}\frac{d(D_nV)}{dt} = K_{td}[P_n^\bullet]\sum_{m=0}^{\infty}[P_m^\bullet] + \frac{K_{tc}}{2}\sum_{m=0}^{n}[P_m^\bullet][P_{n-m}^\bullet],$$

$$n \neq m.$$

$$\frac{d(D_n)}{dt} = K_{td}[P_n^\bullet]\sum_{m=0}^{\infty}[P_m^\bullet] + \frac{K_{tc}}{2}\sum_{m=0}^{n}[P_m^\bullet][P_{n-m}^\bullet],$$

$$n \neq m. \quad (4.17)$$

4.2 Methodology

Chain growth polymerization reactions like the case of FRP of Styrene to Polystyrene are usually computationally intensive simulations which usually take hours or even days to complete. Several factors among others are responsible for a long period of computations such as increasing chain length, kinetic constants, and robustness of computational techniques or algorithms deployed and so on. This is again highlighted in the fact that the chemical reaction in this case study consists of both fast and slow chain reactions as the polymerization possibly progresses through the gel, glass, and cage stages of the chemical reaction.

Hence, a Hybrid Stochastic Simulation Algorithm (HSSA) was used in simulating the FRP reaction system in this project. The idea behind the choice of the HSSA was to take care of the shortcomings associated with the computational efficiency of the older versions of the Gillespie algorithm as well as exploit the advantages of the same. (D.T. GILLESPIE, 2007) In addition, a high average chain length of up to 10^5 can be captured in the algorithm using the gillepsy2 software which upon data processing produced polydispersity indices (PDI) which were in agreement with the experimental results as well as literature.

As shown in the proposed research workflow in Figure (4.1) below, the HSSA allows parallel simulations of both stochastic and deterministic simulations to run concurrently when using the gillespy2 python library. (DRAWERT et al., 2017) The deterministic profiles were obtained by using an Ordinary Differential Equation (ODE) solver with C^{++} dependencies which were compared with the corresponding stochastic trajectories of the same reaction system.

As illustrated to the Figure 4.1 below, the workflow of the computations carried-out in this project was divided into two (2) stages: (**I**) Parallel simulations and, (**II**) Further Computations. To begin, the parallel simulation was carried-out as described in the HSSA steps in Section 4.3 for both stochastic and deterministic computations based on the input conditions described in the Table of simulation results in Chapter 5.

Referring to the second stage of the work flow, the datasets obtained from the parallel simulation were prepared and further computations were carried-out to obtain the polymer's end-use properties such as monomer conversion rate (X), polydispersity index (PDI), Number - Average molecular mass (Mn) and, Weight - Average molar mass (Mw).

The obtained results were compared with experimental results. If the results are not within the limits of predefined acceptability then, the process is repeated by tuning the input parameters. Otherwise, the results or information obtained can be utilized for large scale decision-making.

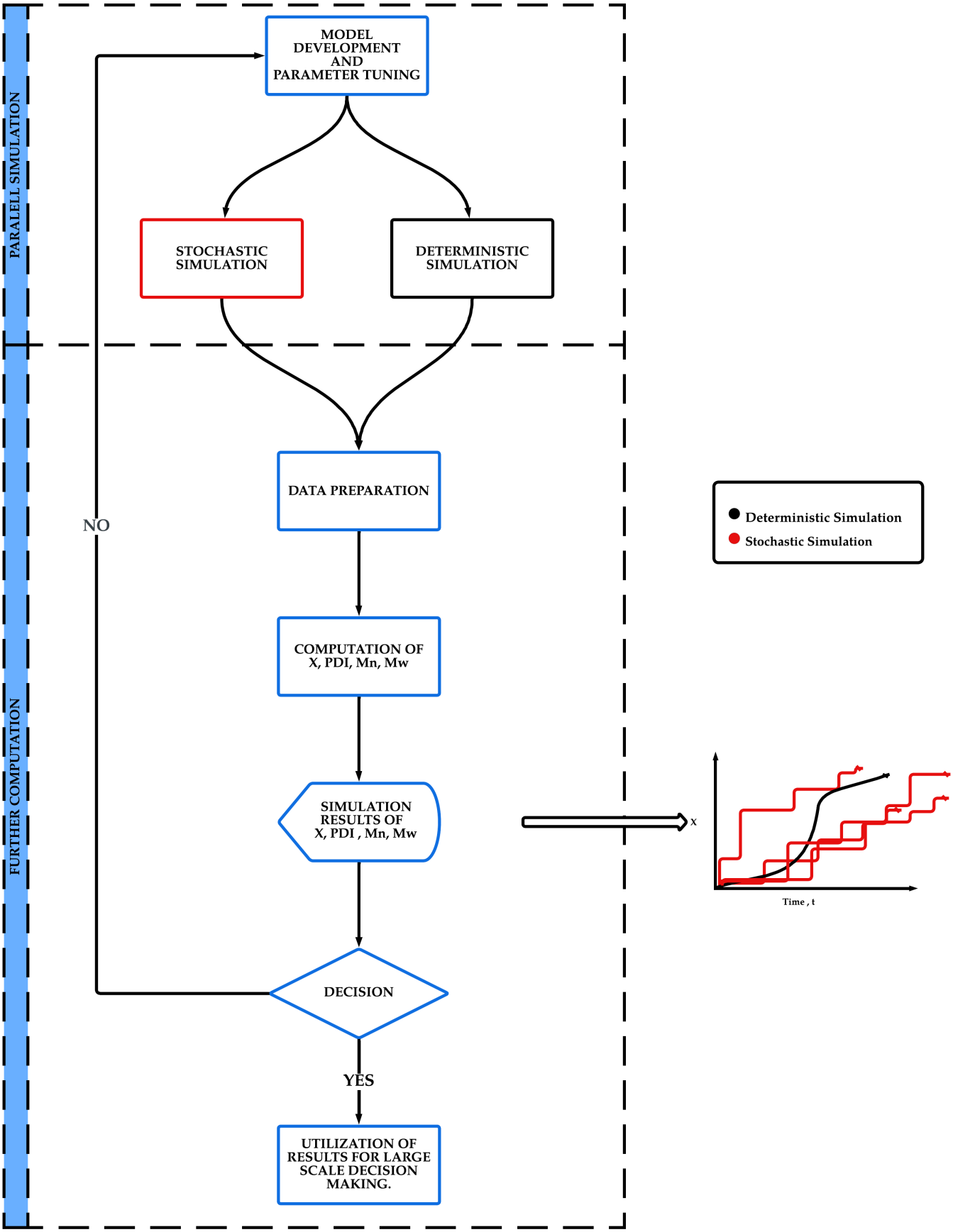

Figure 4.1: A proposed workflow or framework for the application of the Hybrid Stochastic Simulation Algorithm (HSSA).

In order to validate the proposed HSSA model, varying operating temperatures of 100 and 115 degrees Celsius as well as different feeding conditions of monomer, solvent and initiator concentrations were introduced as used in the benchmark experiment earlier carried out. The polydispersity index (PDI), monomer conversion (X), and molecular weight distribution (MWD) were obtained.

The experimental kinetic constants used in this project were also reported in the previous experimental work to simulate the FRP of styrene using Syrris ASIA milli-reactor. However, the termination step was assumed to be predominantly by disproportionation as indicated by Equation (4.11) in chapter three. Table (4.2) below shows the kinetics constants used in the stochastic simulation for the given FRP reaction system:

Table 4.2: Table of kinetic constants used for the HSSA

REACTION STEP	KINETIC CONSTANT	UNIT	REFERENCE
Chemical Initiation	$k_d = 1.0272\times\ 10^{17}\exp(-15924/T)$ $\mathrm{k}_i = 0$	s^{-1} $Lmol^{-1}s^{-1}$	(CABRAL et al., 2003)
Thermal Initiation	k_{iterm}=$1.990\times\ 10^{6}\exp(-1.4842\times 10^{4}/T)$	$kg^{-3}m^{-6}s^{-1}$	(CUTTER and DREXLER, 1982)
Chain Propagation	k_p=$1.051\times\ 10^{7}\exp(-3.577\times 10^{3}/T)$	$m^3.kmol^{-1}s^{-1}$	(HUI and HAMIELEC, 1972)
Chain Transfer	$k_{trM} = 3.110\times\ 10^{3}\exp(-5631/T)$ $k_{trS} = 1.968\times\ 10^{4}\exp(-6302/T)$	$kgm^{-3}s^{-1}$ $kgm^{-3}s^{-1}$	(KIM and CHOI, 1989; BAWN, 1987)
Termination by Combination	k_t=$1.255\times\ 10^{9}\exp(-844/RT)$ $k_{tc} = 0 * k_t$	$kgm^{-3}s^{-1}$	(HUI and HAMIELEC, 1972)
Termination by Disproportionation	k_t=$1.255\times\ 10^{9}\exp(-844/RT)$ $k_{td} = 1 * k_t$	$kgm^{-3}s^{-1}$	(HUI and HAMIELEC, 1972)
Initiator Efficiency	f=$0.8991\times\ 10^{2}\exp(-14.24/RT)$	$kJmol^{-1}$	(FROUNCHI, FARHADI, and MOHAMMADI, 2002)

Applying Flory statistical distribution, the molecular weight distribution (MWD), polydispersity index (PDI) and monomer conversion (X) in terms of the dead polymer, D_n when termination is by disproportionation (i.e., $K_{td} + K_{tc} \gg K_{td}$), then the propensity of propagation for the chain growth reaction is given by:

$$\beta = \frac{(Rate\ of\ Propagation)}{(Rate\ of Propagation) + (Rate\ of\ Termination\ by\ Disproportionation)} \tag{4.18}$$

$$\beta = \frac{\left(k_p M R^{\bullet}\right)}{(k_p M R^{\bullet}) + (k_{trM} M R^{\bullet}) + (k_{trS} S R^{\bullet}) + \left(k_{td}\left(R^{\bullet}\right)^2\right)} \tag{4.19}$$

Or:

$$\beta = \frac{(K_p M)}{(K_p M) + (K_{trM} M) + (K_{trS} S) + (K_{td} R^{\bullet})} \tag{4.20}$$

Where $R^{\bullet}$ is the formed radicals in the chain growth reaction.

Considering chain initiation by only chemical initiation and the rate of termination of chain or the net rate of disappearance of radicals of the growing polymer chain:

$$-r_1 = -2 f K_d I_2 - K_{trM} M \sum_{i=2}^{\infty} R_i - K_{trS} S \sum_{i=2}^{\infty} R_i + K_{td} R_1 \sum_{i=1}^{\infty} R_i \tag{4.21}$$

Overall, for a chain length of i, the net rate of disappearance of radicals for $i \geq 2$:

$$-r_i = K_p M (R_i - R_{i-1}) + K_{trM} M R_i + K_{trS} S R_i + K_{td} R_i \sum_{i=1}^{\infty} R_i \tag{4.22}$$

Adding Equation (4.21) and Equation (4.22) above for chain lengths starting from $i = 2 \rightarrow \infty$:

$$\sum_{i=1}^{\infty} -r_i = -2fK_dI_2 + K_{td}R_i \sum_{i=1}^{\infty} R_i \tag{4.23}$$

For the formation of the radicals let:

$$R^{\bullet} \equiv R_i^{\bullet} \equiv P_i^{\bullet} \equiv \sum_{i=1}^{\infty} R_i$$

$$\sum_{i=1}^{\infty} -r_i = -2fK_dI_2 + K_{td}(R^{\bullet})^2 \tag{4.24}$$

Applying Pseudo Steady State Hypothesis (PSSH) the Equation (4.24), the net free radical concentration is given by:

$$\sum_{i=1}^{\infty} -r_i = -2fK_dI_2 + K_{td}(R^{\bullet})^2 = 0 \tag{4.25}$$

Or:

$$R^{\bullet} = (\frac{2K_dfI_2}{K_{td}})^2 \tag{4.26}$$

Upon substituting Equation (4.26) into Equation (4.20) :

$$\beta = \frac{(K_pM)}{(K_pM) + (K_{trM}M) + (K_{trS}S) + (2K_{td}fI_2)^{\frac{1}{2}}} \tag{4.27}$$

The initiator, solvent, styrene monomer, live, and dead polymers are denoted by I, S, M, P, and D respectively. In addition, the respective kinetic constant for initiator dissociation, chemical, thermal initiation, propagation, transfer to monomer, transfer to solvent, termination by combination and disproportionation is K_d, K_i, K_{iterm}, K_p, K_{trM}, K_{trS}, K_{tc} and, K_{td}. The constant f at the chemical initiation reaction step is referred to as the initiator's efficiency, which ranges between $0.2 < f \leq 0.7$. Since, β is a function of time and when chain transfer is negligible then, the monomer conversion rate can simply be obtained assuming $\beta = X$.

Alternatively, for chain growth polymerization:

$$\beta = \frac{Rate\ of\ Propagation}{Rate\ of\ Propagation + Rate\ of\ Termination}$$

Where:

β = probability that a radical on an active chain will propagate rather than terminate.

Again, assuming that $[M], [I]$ are constant at low conversion, probability that a dead chain is an i-mer:

$$P(i) = \beta^{i-1}(1-\beta) \tag{4.28}$$

Where: β^{i-1} = Termination when next monomer is added.

In a similar fashion for the equation below represents the termination of an active growing chain:

$$P(i) = \sum_{j=1}^{i-1} P(j) P(i-j) \tag{4.29}$$

Recall from the above above Equation (4.28) that:

$$P(j) = \beta^{j-1}(1-\beta) \tag{4.30}$$

Then termination by combination becomes:

$$P(i-j) = \beta^{(i-j-1)}(1-\beta) \tag{4.31}$$

Substituting Equation (4.54) and (4.55) into Equation (4.29):

$$P(i) = \sum_{j=1}^{i-1} \left[\beta^{(j-1)+(i-j-1)}(1-\beta)^2\right] \tag{4.32}$$

$$P(i) = \sum_{j=1}^{i-1} (1-\beta)^2 (\beta)^{i-2} \tag{4.33}$$

Finally:

$$P(i) = (i-1)(1-\beta)^2 (\beta)^{i-2} \tag{4.34}$$

It is worth noting that, $P(i)$ which again defines the probability that a dead chain as an i-mer:

$$P(i) = \frac{N_i}{N_T} \tag{4.35}$$

Where:
N_i = total number of dead i-mers. N_T = total number of dead polymer formed.

Therefore:

$$P(i) = \frac{N_i}{N_T} = (i-1)(1-\beta)^2 (\beta)^{i-2} \tag{4.36}$$

$$N_i = N_T (i-1)(1-\beta)^2 (\beta)^{i-2} \tag{4.37}$$

NUMBER MOLECULAR WEIGHT DISTRIBUTION (Mn):

Recall that Mn is given by:

$$Mn = \frac{\sum N_i M_i}{\sum N_i} \tag{4.38}$$

But; $M_i = iM0$ and $N_T = \sum N_i$ then, the previous Equation (4.38) becomes:

$$Mn = \sum \left[\frac{Ni}{N_T} (iM_0) \right] \tag{4.39}$$

Substituting Equation (4.36) into Equation (4.39):

$$Mn = M_0 (1-\beta)^2 \sum i (i-1) \beta^{i-2} \tag{4.40}$$

Furthermore, it can be shown that given that N is large and $|\beta| < 1$:

$$\sum i (i-1) \beta^{i-2} = \frac{2}{(1-\beta)^3} \tag{4.41}$$

Finally by substituting Equation (4.43) into Equation (4.42):

$$Mn = \frac{2M_0}{(1-\beta)} \tag{4.42}$$

WEIGHT MOLECULAR WEIGHT DISTRIBUTION (Mw):
Again by definition;

$$Mw = \frac{\sum N_i M_i^2}{\sum N_i M_i} \tag{4.43}$$

Given that $W_i = N_i M_i$ and $w_i^* = \frac{W_i}{W_T}$ are the respective chain weights and weight fraction of the growing per molecule, then:

$$Mw = \sum \left[\frac{W_i M_i}{W_T}\right] \tag{4.44}$$

$$Mw = \sum \left[\left(\frac{N_i M_i}{W_T}\right)(iM_0)\right] = \sum \left[\frac{W_i}{W_T}(iM_0)\right] \tag{4.45}$$

Considering the Chain Termination events:

For Chain Disproportionation Reaction Step:

$$\beta = 1 - \frac{N_T}{N_0} \tag{4.46}$$

For Chain Combination Termination Reaction Step:

$$\beta = \frac{N_0 - N_T}{N_0} = \beta = 1 - \frac{2N_T}{N_0} \tag{4.47}$$

Again,substituting Equation (4.47) into Equation (4.37):

$$N_T = \frac{N_0}{2}(1-\beta)^3 (i-1)\beta^{i-2} \tag{4.48}$$

Substituting the above Equation (4.48) into Equation (4.45):

$$Mw = \sum \frac{iM_0 \frac{N_0}{2} (1-\beta)^3 (i-1) \beta^{i-2} iM_0}{N_0 M_0} \tag{4.49}$$

$$Mw = \frac{M_0}{2} (1-\beta)^3 \sum i^2 (i-1) \beta^{i-2} \tag{4.50}$$

Again, it can be shown that if N is large, and $|\beta| < 1$:

$$\sum_{i=1}^{N} i^2 (i-1) \beta^{i-2} = \frac{2(2+\beta)}{(1-\beta)^4} \tag{4.51}$$

Substituting Equation (4.51) into Equation (4.50):

$$Mw = M_0 \frac{(2+\beta)}{(1-\beta)} \tag{4.52}$$

POLYDISPERSITY INDEX (PDI):

In order to obtain the corresponding mathematical expression for the Polydispersity Index, Equation (4.52) is divided by Equation (4.42):

$$PDI = \frac{Mw}{Mn} = \frac{2+\beta}{2} \tag{4.53}$$

Error Calculation:

Given the benchmark experimental values (FULLIN et al., 2015) and the obtained simulation results discussed in the next chapter, the absolute error or deviations, E and Percentage Relative Error, $E\%$ are calculated as follows:

$$E = |E_i - S_i| \tag{4.54}$$

$$E\% = \left| \frac{E_i - S_i}{E_i} \right| \ X100\% \tag{4.55}$$

Where, $i = 1, 2, 3, \ldots, N$

Another statistical tool for validating the numerical simulation outcomes is the Average Percentage Error (APE) to measure the accuracy of the monomer conversion rate (X) and polydispersity index (PDI) obtained from the HSSA simulation.

The Average Percentage Error (APE) is computed as follows:

$$APE = \left(\frac{1}{n}\right) * \sum \frac{|E_i - S_i|}{|E_i|} \ X100\% \tag{4.56}$$

4.3 Application of the Hybrid Stochastic Simulation Algorithm (HSSA)

Hybrid Stochastic Simulation Algorithms (HSSA) are variants or a subset of the Stochastic Simulation Algorithms (SSA) that integrate the functionalities of two or more variants depicted in the classification tree in Figure (3.2) of the SSA to increase the speed of computation, as well as the robustness to solve complex chemical reactions. As earlier stated, the inherent stochasticity of these chemical reactions is interpreted based on the principles of the Chemical Master Equation (CME). In this context, each of the possible reaction channels or sub-reactions is interpreted by the CME which comprises both slow and fast dynamics in the entire chemical reaction as the chain propagation progresses and then, terminates. Hence, the choice of the HSSA is based on the context of the problem at hand. (HSSA, 2022)

As earlier introduced in Chapter 3, Haseltine and Rawlings (2002) proposed the HR algorithm or the Hybrid Stochastic Simulation Algorithm (HSSA) with a framework close to the one adopted in this work. (HASELTINE and RAWLINGS, 2002) It aims at improving accuracy and increasing computational speed by partitioning the reaction into fast and slow components or simply by applying "Stochastic Partitioning".

Generally, an ODE is represented by:

$$\frac{dx(t^{'})}{dx} = f(x(t^{'})) \tag{4.57}$$

Upon manipulating Equation (3.8) and equation (3.4) within a time of $t \rightarrow t + \tau$:

$$P(\tau, j) = c_j h_j d\tau exp(-\int_t^{t+\tau} c_j h_j dt) \tag{4.58}$$

Alternatively:

$$P(\tau, j) = \alpha_j d\tau exp(-\int_t^{t+\tau} \alpha_j dt) \tag{4.59}$$

Considering Equation (3.14) and upon further mathematical manipulation, the time for the next reaction and the corresponding propensity to occur are given by:

$$\int_t^{t+\tau} \alpha_j(x(t^{'}))dt^{'} + \ln \xi_1 = 0 \tag{4.60}$$

Where $t^{'}$ is the time taken for a corresponding "slow" reaction to take place.

It is worth noting according to the HR algorithm, the computation of the "fast" reactions of the partitioned chemical reaction system takes place within the infinitesimal time, $t^{'}$ according to the above Equation (4.60). Notwithstanding, the LSODA solver from the SciPy python library was used in this project which is also capable of computing DAEs of index 1.

As shown in the computational steps below, the gillespy2 python module used was earlier developed by Drawert et al. (2017). (DRAWERT et al., 2017) The program allows the parallel simulation of both the stochastic and deterministic simulation of the FRP of the styrene model. With C^{++} integration, version 1.8.2 of the gillespy2 python library is computationally robust and scalable for a number of complex chemical reaction systems such as the FRP with chain lengths of up to 2^{31} - 1 per macromolecule.

The deterministic profiles obtained from every simulation produced were compared with every stochastic trajectories generated. Usually, analytical solutions for a complex chemical reaction system such as the FRP of styrene produce over 100,000 stiff ODEs. Moreover, with approximate methods like the application of Methods of Moments (MoM), these large sets of ODEs are reduced to a fewer number of non-stiff differential equations or differential algebraic equations (DAEs) of index 1. This reduces the accuracy of the prediction of the polymer's end-use properties. Nonetheless, it is worth noting that the HSSA used in this work combines ODE and SSA solvers for the chain growth reaction mechanism for every propensity change without partitioning the system. It can be further employed to track the polymer's end-use properties for an increasing number of chain lengths. However, in this work, the maximum chain length simulated per macromolecule was limited to 100 chains per macromolecule based on the computing capacity of the computer.[1]

Furthermore, for wider scale applications, when considering Free Radical Polymerization or Chain Growth Polymerization, the transition from microscopic to macroscopic scale occurs as a function of the number of molecular reacting species (i.e., monomer) initiating the polymerization reaction mechanisms. Another key factor is the reaction volume (a volume of $4mL$ is used in this study). Thus, for small volume systems, a stochastic algorithm finds its application useful in this case.

Generally, as elaborated in Section 4.3, stochastic simulation algorithms track each reaction mechanism (taking into account of molecular species concentration and

[1]All performed simulations were carried out using the computational architecture: Windows intel (R) i5-M480, 500GB of DDR4, 2.67GHZ RAM 4GB.

kinetic constant) of the growing chain by computing the propensity of each reaction step in addition to calculating a number "r" from a uniform random distribution $U(0,1)$.

The Hybrid Stochastic Simulation Algorithm or HSSA is illustrated in the following steps below. The stochastic and deterministic computation for the FRP model were carried-out in **STEP 5** and **STEP 8** respectively. It is also worth noting that in **STEP 6**, the tau-leaping algorithm was deployed to simulate an ensemble of 100 stochastic trajectories which was also used in the analysis.

STEP 1 Initiate the FRP of the Styrene model according to the chemistry of reaction in the Table (4.1) using gillespy2. Next, define the microchannel volume and input the reaction parameters.

STEP 2 By applying the stochastic constants, c_j from the Table (3.1), compute the respective cumulative propensities for each of the chain reaction, R_j by using the equation :

$$\alpha_j = \sum_j c_j h_j$$

Where $j = (1, 2, 3, \ldots, N)$ and h_j is the number of instant combinations of reactants for reaction, R_j.

STEP 3 Generate two pseudo-random numbers ξ_1 , ξ_2 from a Uniform Random Distribution (URD) or $\sim U(0,1)$.

STEP 4 Initiate the stochastic simulation according to Equations (3.14) and (3.16) for the next reaction time and propensity at $t \to t + \tau$.

STEP 5 Update the chemical reaction system such that:

$$t \leftarrow t + \tau \;\; and \;\; X \leftarrow X + v_{ij}$$

The iteration continues until the number of iterations n exceeds the simulation time, t_f where: $n > t_f$
Else:
Repeat **STEP 3**

STEP 6 Initiate the stochastic simulation to generate an ensemble of 100 stochastic trajectories according to the Equations used in **STEP 4** and Equation (3.17) for the next reaction time and propensity at $t \to t + \tau$ given that:

$$\lambda = \frac{e^{-\alpha_j(x)\tau} \left(\alpha_j(x)\tau\right)^k}{k!}$$

STEP 7 Update the chemical reaction system such that:

$$t \leftarrow t + \tau \;\; and \;\; X \leftarrow X + \lambda$$

The iteration continues until the number of iterations n exceeds the simulation time, t_f where: $n > t_f$
Else:
Repeat **STEP 3**

STEP 8 Initiate the deterministic simulation by integrating the ODEs developed from the reaction for every occurring reaction channel, R_j according to Equations used in **STEP 4**.

STEP 9 Data Processing and Computation of the values of X, Mn, Mw, and PDI using Equation (4.28) to Equation (4.55).

The results obtained from the simulation are further discussed in the "Results and Discussions" chapter of this project. Also, the code used in this project can be found in GitHub repository.[2]

[2]Project Code

CHAPTER 5
RESULTS AND DISCUSSIONS

5.1 Results of the HSSA

The FRP of Styrene was carried out by adhering to the same feeding conditions in the experiment performed by Fullin et al. (2015) to validate the HSSA. The feeding conditions and operating temperatures used are shown in Tables (5.1), (5.2) and (5.3). Moreso, the styrene monomer was polymerized in a Syrris Asia 120 microreactor with a volume of $4mL$. Thus, the reacting volume adapted in the simulation is also the same. In addition, the similar set of kinetic values used in the HSSA simulation were also reported from the referenced experiment as shown in Table (4.2). (FULLIN et al., 2015)

For completeness, the referenced experimental work and the simulation results which were obtained from the parallel simulation capabilities of the HSSA simulation outcomes were compared. The results generated as shown in Tables (5.1), (5.2) and (5.3) were used to validate the proposed HSSA model. Furthermore, by applying the same operating conditions used in the experimental work of Fullin et.al (2015) according to tables presented below which were the mass of the monomer, solvent and initiator as well as operating temperatures, the HSSA provided a very good agreement with experimental results. In addition, within a simulation time of 20 to 80 minutes, the Average Percentage Errors or APEs for both the Monomer Conversion (X) and Polydispersity Index (PDI) were 23.27%, 11.83% and 20.04%, 13.24% for this work and the referenced experiment respectively in terms of the deterministic simulations carried-out. However, referring to Table (5.1), while the HSSA produced agreeable outcomes for the Polydispersity Index (PDA) and the molecular weight distributions (Mn and Mw) for the first five 5 minutes of the simulation, the monomer conversion rate (X) was twice that of the experiment.

As shown in the tables, the stochasticity of the model was not captured within the conditions used in the experiment. Moreso, as reported in the work of Fullin et.al (2015), the graphs of the rate of monomer conversion, polydispersity and the number and weight average molar masses showed no perturbation within the conditions. This

implied that there was no clogging of the milli-reactor pores and also, the monomer, solvent and initiator were well-mixed within the reactor.

Table 5.1: A Comparative Table of Results from the Hybrid Stochastic Simulation Algorithm (HSSA) and Experimental Results from FULLIN et al., 2015

Table of Results for Mn, Mw, PDI and X Operating Temperature, T = 100°C											
DETERMINISTIC SIMULATION*				STOCHASTIC SIMULATION*				EXPERIMENTAL RESULTS*			
Mn	Mw	PDI	X	Mn	Mw	PDI	X	Mn	Mw	PDI	X
10008	14908	1.49	0.18	-	-	-	-	6768	13607	1.57	0.091
DETERMINISTIC SIMULATION**				STOCHASTIC SIMULATION**				EXPERIMENTAL RESULTS**			
Mn	Mw	PDI	X	Mn	Mw	PDI	X	Mn	Mw	PDI	X
6384	9471	1.49	0.24	-	-	-	-	5640	8223	1.68	0.391

* M/S = 60/40 v/v OR 41g / 59g ; I = 1g Simulation Time, t = 5 mins.

** M/S = 60/40 v/v OR 41g / 59g ; I = 1g Simulation Time, t = 20 mins.

Table 5.2: A Comparative Table of Results from the Hybrid Stochastic Simulation Algorithm (HSSA) and Experimental Results from FULLIN et al., 2015

Table of Results for Mn, Mw, PDI and X Operating Temperature, T = 100°C											
DETERMINISTIC SIMULATION *				STOCHASTIC SIMULATION *				EXPERIMENTAL RESULTS *			
Mn	Mw	PDI	X	Mn	Mw	PDI	X	Mn	Mw	PDI	X
11440	17055	1.49	0.36	-	-	-	-	10264	16313	1.59	0.411
DETERMINISTIC SIMULATION **				STOCHASTIC SIMULATION **				EXPERIMENTAL RESULTS **			
Mn	Mw	PDI	X	Mn	Mw	PDI	X	Mn	Mw	PDI	X
10354	15427	1.49	0.41	-	-	-	-	14169	23337	1.65	0.61

* M/S = 40/60 v/v OR 61g / 39g ; I = 1g Simulation Time, t = 40 mins.

** M/S = 40/60 v/v OR 61g / 39g ; I = 1g Simulation Time, t = 80 mins.

Table 5.3: A Comparative Table of Results from the Hybrid Stochastic Simulation Algorithm (HSSA) and Experimental Results from FULLIN et al., 2015

Table of Results for Mn, Mw, PDI and X Operating Temperature, T = 115°C											
DETERMINISTIC SIMULATION *				STOCHASTIC SIMULATION *				EXPERIMENTAL RESULTS *			
Mn	Mw	PDI	X	Mn	Mw	PDI	X	Mn	Mw	PDI	X
10510	15661	1.49	0.42	-	-	-	-	8512	15603	1.83	0.653
DETERMINISTIC SIMULATION **				STOCHASTIC SIMULATION **				EXPERIMENTAL RESULTS **			
Mn	Mw	PDI	X	Mn	Mw	PDI	X	Mn	Mw	PDI	X
22282	33319	1.50	0.40	-	-	-	-	26088	50576	1.94	0.524

* M/S = 70/30 v/v OR 70.9g / 29.1g ; I = 1g Simulation Time, t = 80 mins.

** M/S = 70/30 v/v OR 70.9g / 29.1g ; I = 0.5 g Simulation Time, t = 80 mins.

5.1.1 Deterministic Versus Stochastic simulation Results.

Again, in this work, the feeding ratios of the monomer, solvents and initiator were increased with a multiplicative scale factor k as shown in Tables (5.4), (5.5) and (5.6) in order to further test HSSA. In addition, the operating temperature, T, was also increased to 140°C in order to reduce viscosity, increase the reaction rates and also improve overall polymer properties. (Jafarzadeh-Kashi et al., 2011; Nising, 2006)

The graphical plots in the Figures shows the resulting outcomes of the Hybrid Stochastic Simulation Algorithm (HSSA) illustrated in Section 4.3. Throughout the simulations carried out, three (3) separate stochastic simulation trajectories were generated, and an ensemble of 100 stochastic trajectories was also generated using the Tau-Leaping algorithm. Also, the corresponding deterministic trajectory of the same chemical reaction system was also generated.

Table 5.4: Deterministic Versus Stochastic simulation Results.

Table of Results for Mn, Mw, PDI and X Operating Temperature, T = 140°C Multiplicative Scale Factor, k = 10^2							
DETERMINISTIC SIMULATION *				STOCHASTIC SIMULATION *			
Mn	Mw	PDI	X	Mn	Mw	PDI	X
1257	1782	1.42	0.96	1609	2309	1.43	0.40
DETERMINISTIC SIMULATION **				STOCHASTIC SIMULATION **			
Mn	Mw	PDI	X	Mn	Mw	PDI	X
978	1364	1.39	0.97	1024	1432	1.40	0.52

* M/S = 60/40 v/v OR 41g / 59g ; I = 1g Simulation time, t = 30 mins.

** M/S = 60/40 v/v OR 41g / 59g ; I = 1 g Simulation time, t = 60 mins.

Table 5.5: Deterministic Versus Stochastic simulation Results.

Table of Results for Mn, Mw, PDI and X Operating Temperature, T = 140°C Multiplicative Scale Factor, k = 10^2							
DETERMINISTIC SIMULATION*				STOCHASTIC SIMULATION*			
Mn	Mw	PDI	X	Mn	Mw	PDI	X
1455	2079	1.43	0.97	1013	1414	1.40	0.54
DETERMINISTIC SIMULATION**				STOCHASTIC SIMULATION**			
Mn	Mw	PDI	X	Mn	Mw	PDI	X
1163	1640	1.41	0.98	627	837	1.33	0.65

* M/S = 40/60 v/v OR 61g / 39g ; I = 1g Simulation time, t = 30 mins.

** M/S = 40/60 v/v OR 61g / 39g ; I = 1 g Simulation time, t = 60 mins.

Table 5.6: Deterministic Versus Stochastic simulation Results.

Table of Results for Mn, Mw, PDI and X Operating Temperature, T = 140°C Multiplicative Scale Factor, k = 10^2							
DETERMINISTIC SIMULATION*				STOCHASTIC SIMULATION*			
Mn	Mw	PDI	X	Mn	Mw	PDI	X
1526	2185	1.43	0.97	819	1125	1.37	0.59
DETERMINISTIC SIMULATION**				STOCHASTIC SIMULATION**			
Mn	Mw	PDI	X	Mn	Mw	PDI	X
1235	1748	1.42	0.98	517	671	1.30	0.70

* M/S = 30/70 v/v OR 70.9g / 29.1g ; I = 1g Simulation time, t = 30 mins.

** M/S = 30/70 v/v OR 70.9g / 29.1g ; I = 1g Simulation time, t = 60 mins.

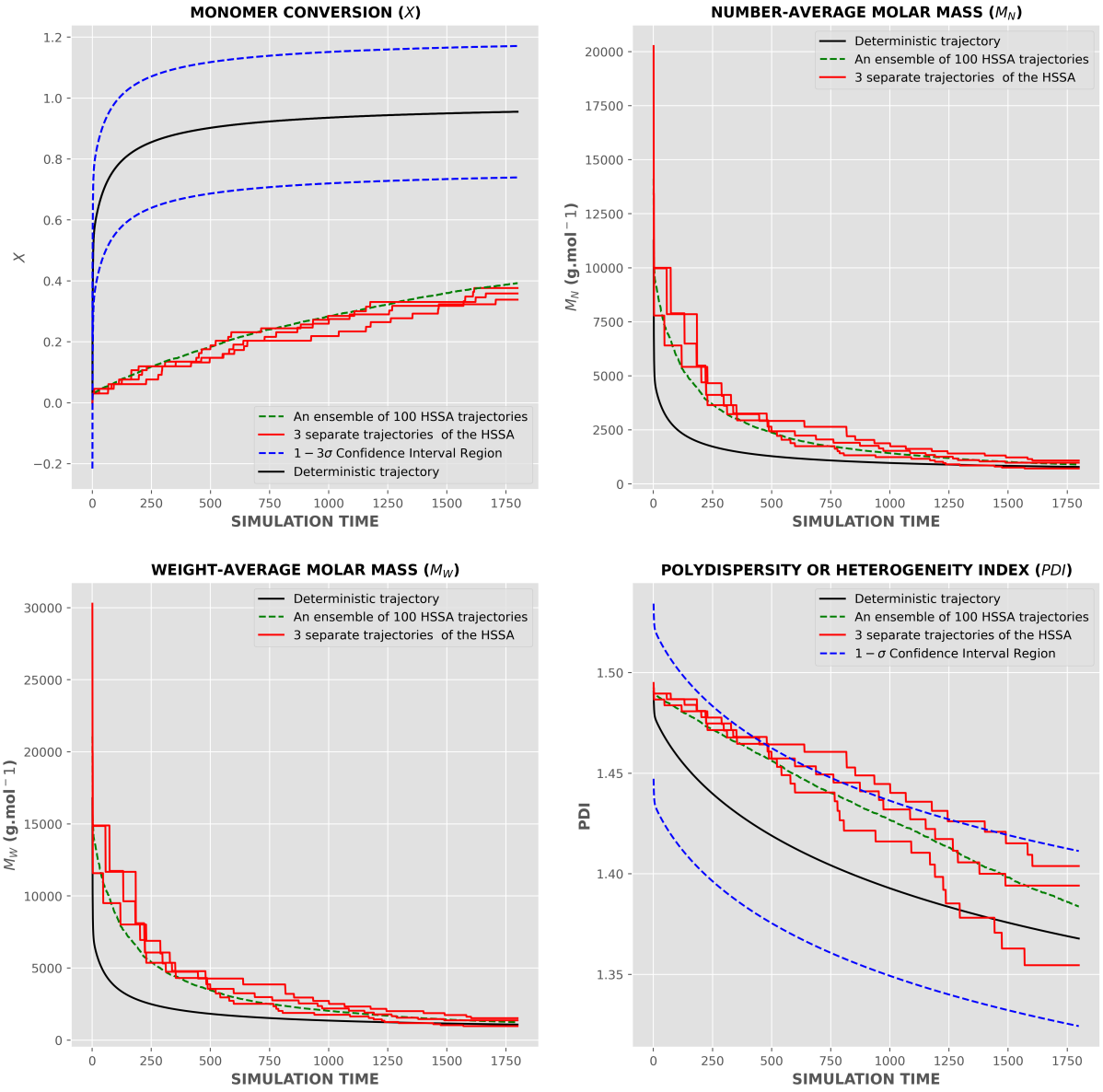

Figure 5.1: A graphical plot of the stochastic trajectories versus the corresponding deterministic profiles of the FRP of Styrene in microchannel (4mL). The green dashes line represents an ensemble of 100 stochastic trajectories. The initial value of Monomer (M) to Solvent (S) in grammes = 41g/59g and Initiator (I) = 1g. Operating Temperature, T = 140°C, time = 30 mins and Multiplicative Scale Factor, k = 10^2.

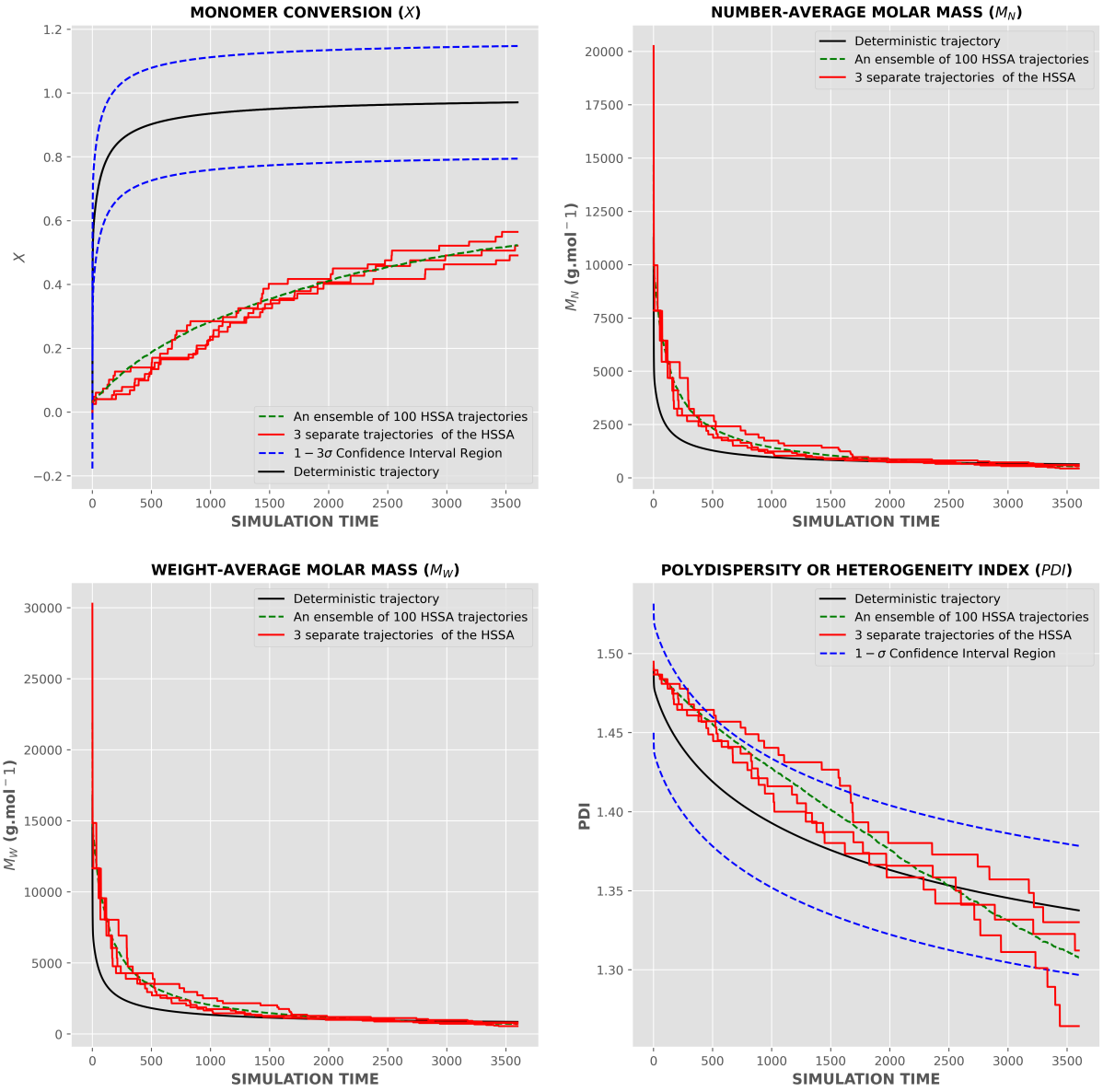

Figure 5.2: A graphical plot of the stochastic trajectories versus the corresponding deterministic profiles of the FRP of Styrene in microchannel (4mL). The green dashes line represents an ensemble of 100 stochastic trajectories. The initial value of Monomer (M) to Solvent (S) in grammes = 41g/59g and Initiator (I) = 1g. Operating Temperature, T= 140°C, time= 60 mins and Multiplicative Scale Factor, k = 10^2.

The graph in Figure (5.1) above, shows a plot of stochastic versus deterministic simulations using the HSSA for the FRP model. In this work, the simulation was carried-out for 30 and 60 minutes along with the conditions stipulated in Table (5.4). As shown in the graphs above, there are deterministic profiles representing the FRP chemical reaction reaction and its corresponding stochastic trajectories as illustrated. For the stochastic trajectories generated, there are 3 separate trajectories representing the FRP system denoted by red stochastic lines. Also, an ensemble of 100 stochastic trajectories were also generated using the Tau-Leaping technique to further validate the stochastic simulation.

In addition, confidence interval plots based on the deterministic profiles were only plotted for the monomer conversion rate (X) and polydispersity index (PDI) due to the deviations generated as denoted by the blue dashed lines. Moreover, it can be seen that based on the conditions stipulated in Table (5.4), the stochastic trajectories generated for the monomer conversion rate (X) were deviated from the corresponding deterministic profile. However, for another additional 30 minutes the deterministic profile and the corresponding stochastic trajectories become more aligned as the deviation decreased as shown in Figure (5.2). Notwithstanding, when considering the polydispersity index (PDI), number average molecular mass (Mn) and weight average Molecular mass (Mw) from Figures (5.1) and (5.2), the deterministic profiles and the corresponding stochastic trajectories were more aligned.

Furthermore, referring to Figure (5.2), the stochastic trajectories and the corresponding deterministic profile were more aligned for the monomer conversion rate (X) when compared to Figure (5.1). Although, the stochastic trajectories including the ensemble of 100 stochastic trajectories and the 3 separate stochastic trajectories deviated from the deterministic graphical profile, they were within the three standard deviation envelope or confidence interval . Again, the number average molecular mass (Mn) and weight average molecular mass (Mw) were more aligned based on the conditions stated in Table (5.4). Once again, it can be projected that with a higher simulation time, the stochastic trajectories would align more with the deterministic profile for the monomer conversion rate (X). However, the MWD also becomes narrower with the increment of simulation time. All in all, the results of the MWD obtained based on the conditions of Table (5.4), recorded less deviation thus,the graphical outcome were more aligned as a result when compared to the results recorded in Tables (5.5) and (5.6).

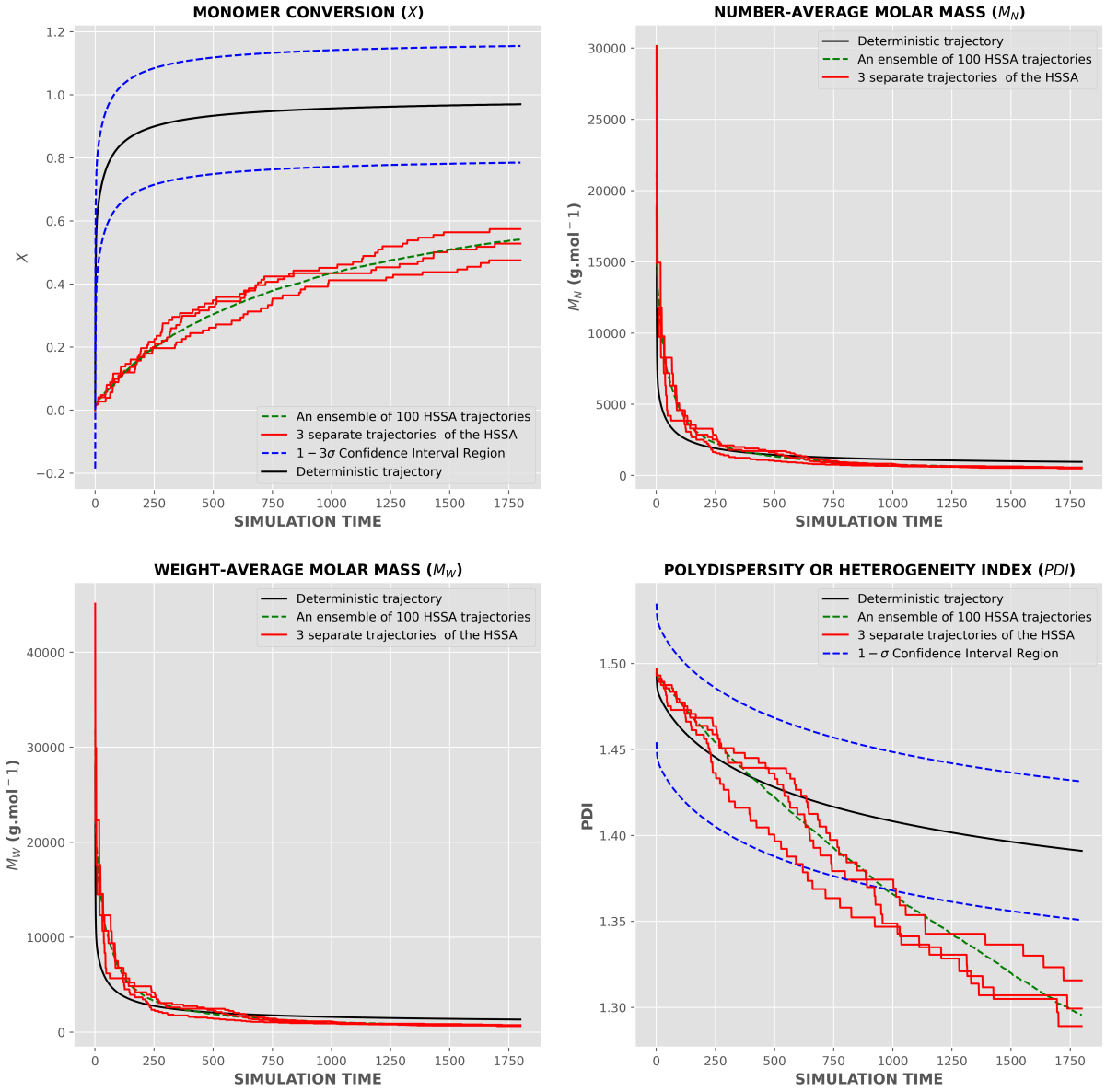

Figure 5.3: A graphical plot of the stochastic trajectories versus the corresponding deterministic profiles of the FRP of Styrene in microchannel (4mL). The green dashes line represents an ensemble of 100 stochastic trajectories. The initial value of Monomer (M) to Solvent (S) in grammes = 61g/39g and Initiator (I) = 1g. Operating Temperature, T = 140°C, time = 30 mins and Multiplicative Scale Factor, k = 10^2.

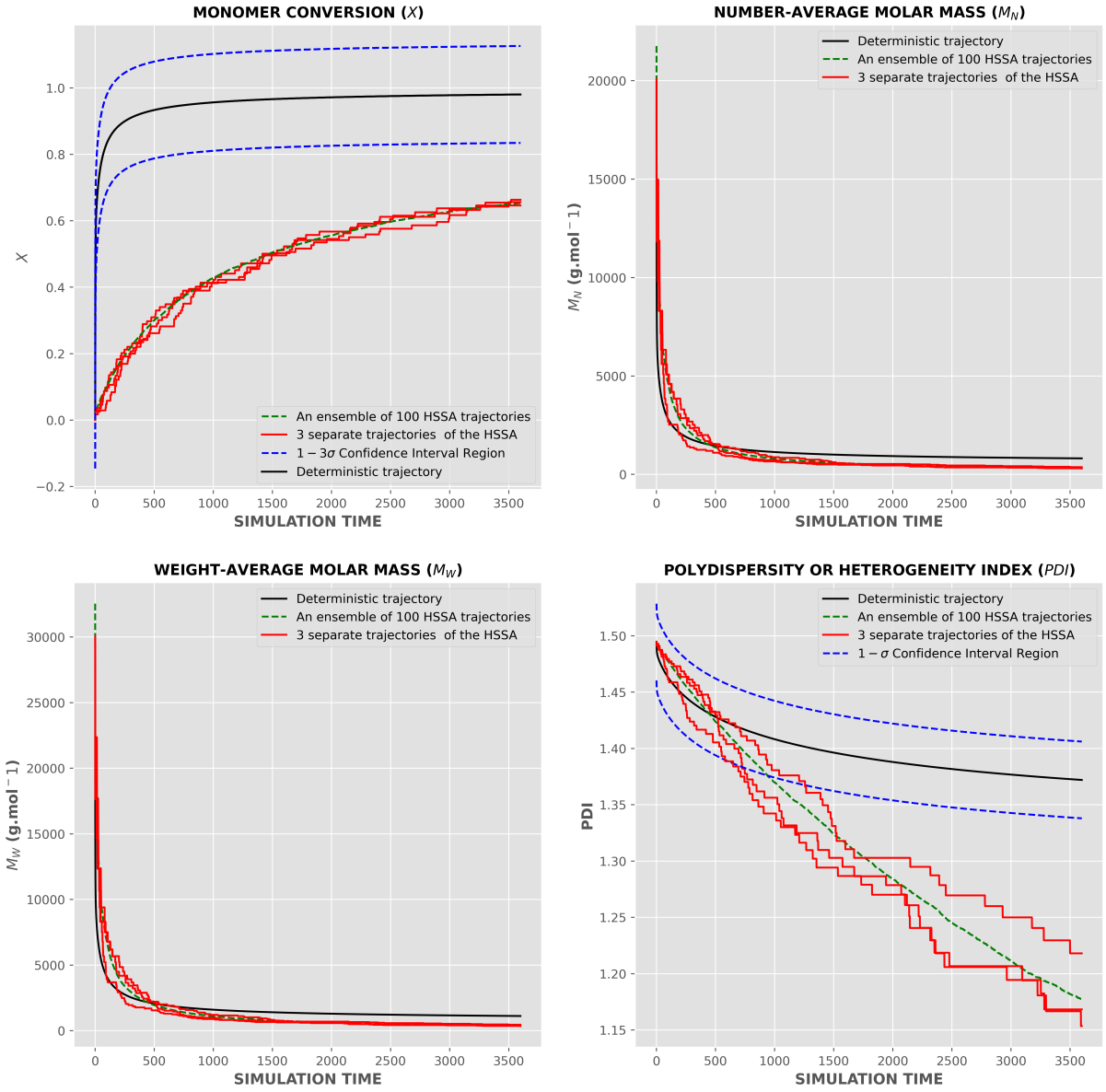

Figure 5.4: A graphical plot of the stochastic trajectories versus the corresponding deterministic profiles of the FRP of Styrene in microchannel (4mL). The green dashes line represents an ensemble of 100 stochastic trajectories. The initial value of Monomer (M) to Solvent (S) in grammes = 61g/39g and Initiator (I) = 1g. Operating Temperature, T = 140°C, time = 60 mins and Multiplicative Scale Factor, k = 10^2.

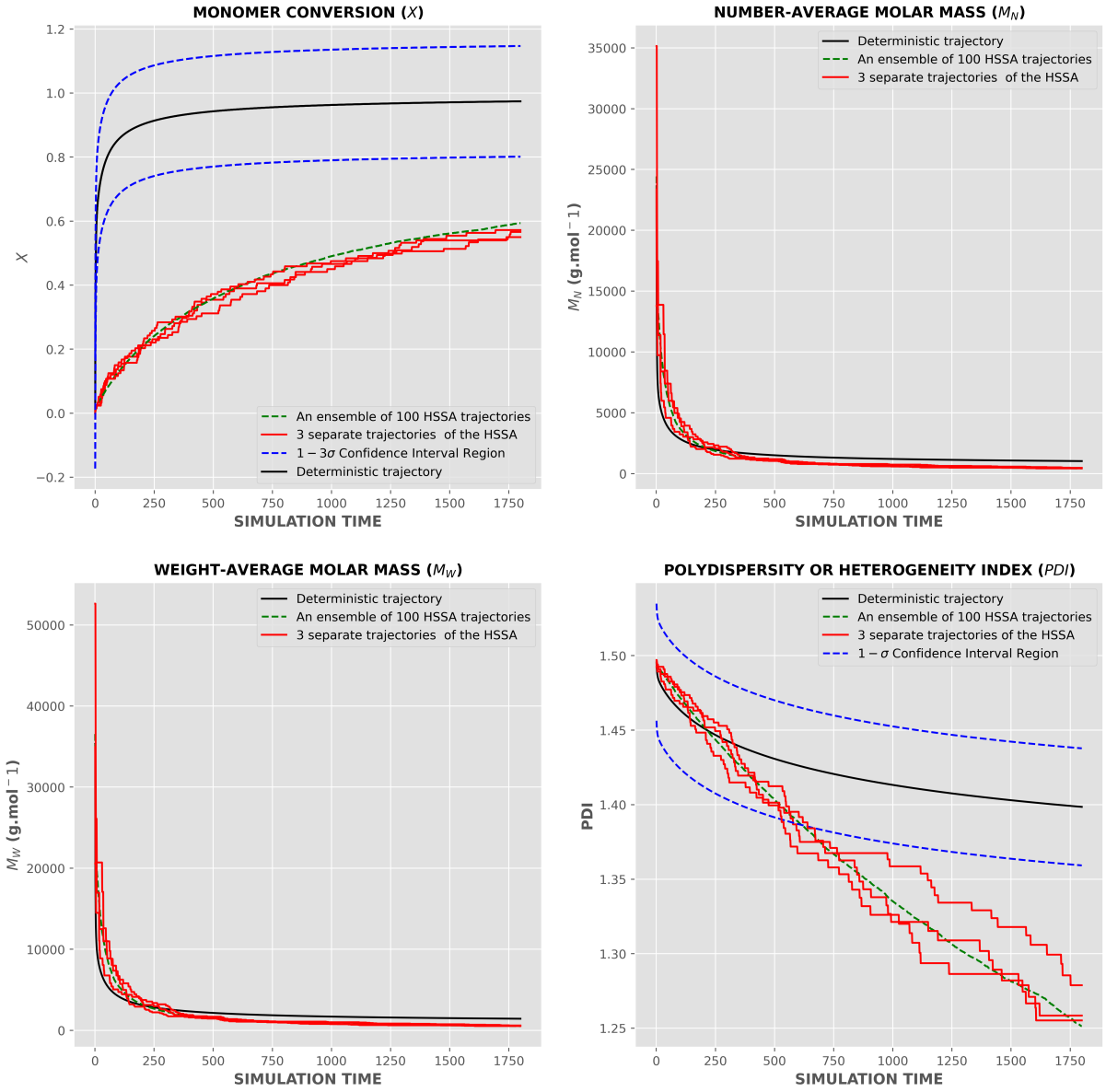

Figure 5.5: A graphical plot of the stochastic trajectories versus the corresponding deterministic profiles of the FRP of Styrene in microchannel (4mL). The green dashes line represents an ensemble of 100 stochastic trajectories. The initial value of Monomer (M) to Solvent (S) in grammes = 29.1g/70.9g and Initiator (I) = 1g. Operating Temperature, T = 140°C, time = 30 mins and Multiplicative Scale Factor, k = 10^2.

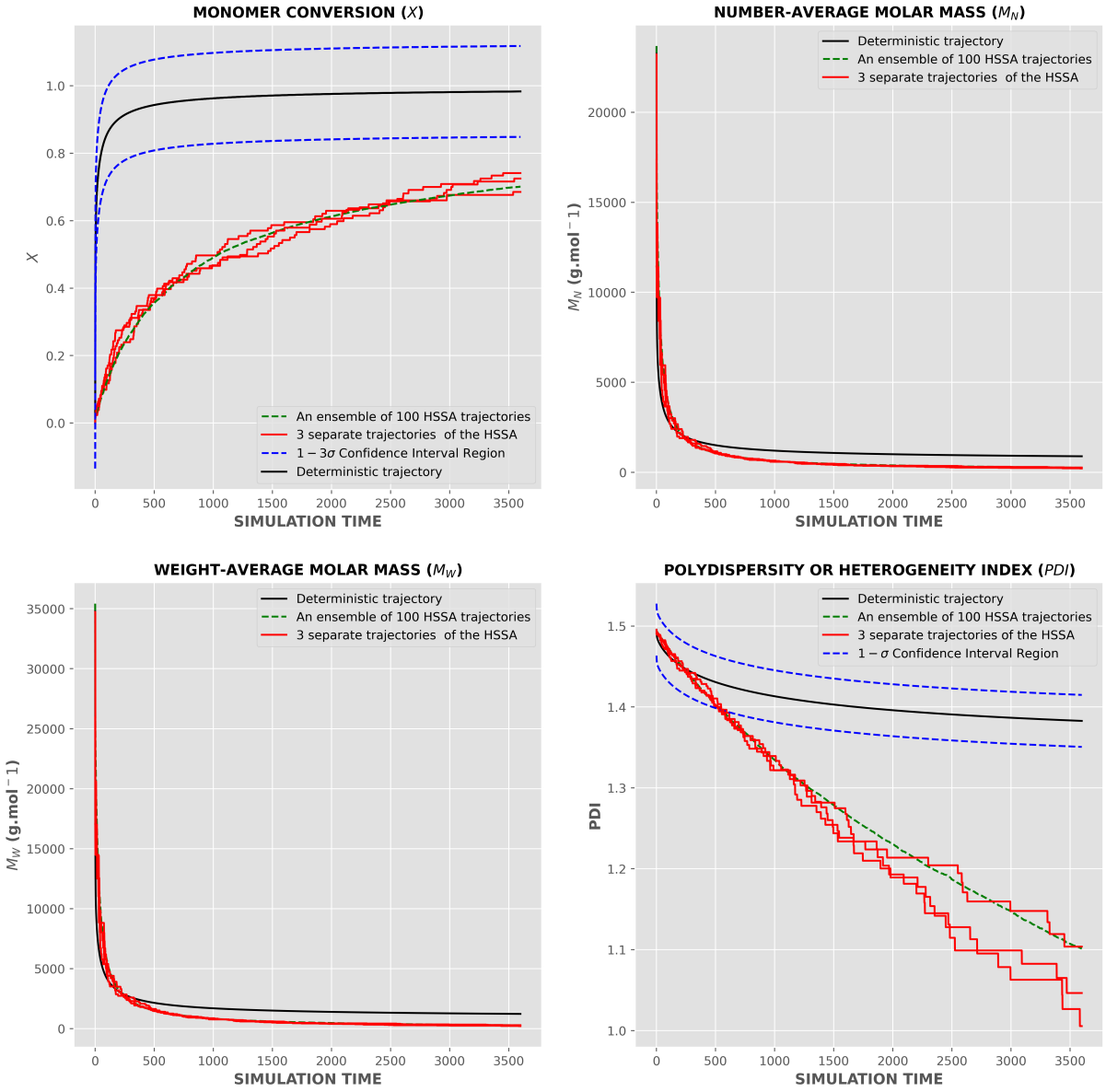

Figure 5.6: A graphical plot of the stochastic trajectories versus the corresponding deterministic profiles of the FRP of Styrene in microchannel (4mL). The green dashes line represents an ensemble of 100 stochastic trajectories. The initial value of Monomer (M) to Solvent (S) in grammes = 29.1g/70.9g and Initiator, (I) = 1g. Operating Temperature, T = 140°C, time = 60 mins and Multiplicative Scale Factor, k = 10^2.

Similarly, referring to Figures (5.3), (5.4), (5.5) and (5.6) as well as adhering to the conditions in the Table (5.5) and Table (5.6), the stochastic trajectories were more aligned when considering the monomer conversion rate (X) thus, this reveals that a higher amount of the styrene monomer resulted to higher conversion rates with the same operating temperature of 140°C. However, as seen in Tables (5.5) and (5.6), the PDIs values resulted in more disparity between the deterministic and stochastic simulations. Notwithstanding, as shown in Figures (5.3), (5.4), (5.5) and (5.6), the generated results agreed closely for both the stochastic and deterministic simulation outcomes in terms of the molecular weight distribution or MWD. Furthermore, the PDIs from both the stochastic and deterministic simulation were more deviated from one another as shown in

the illustrated figures above. The deviations in terms of the PDI were more pronounced when considering Figures (5.5) and (5.6) as the stochastic trajectories were out of the confidence interval plot. Conclusively, this reveals that the conditions in Table (5.4) provided the best monomer to solvent input ratio when compared to Tables (5.5) and (5.6).

5.1.2 Discussions of Simulated Results

The obtained results of the end-use properties of polystyrene such as monomer conversion rate (X), polydispersity index (PDI), number-average molar mass (Mn) and the weight-average molar mass (Mw) were compared to experimental data. With residence times of 30 to 60 minutes, varying operating conditions of initial monomer (M), solvent (S) and initiator (I), as well as an operating temperature of 140°C were implemented.

As for the monomer conversion rates (X), conversion values of 96% to 99% were obtained from the deterministic simulation based on input conditions in Table (5.4),(5.5) and (5.6). Moreso, the main factors responsible for the high values were the operating temperature and increased input values due to the multiplicative scale factor, k . While the corresponding stochastic values for the monomer conversion (X) were less at 40% to 70% , the values are projected to increase with respect to simulation time as well as increased relative monomer mass based on the outcomes shown in Tables (5.4),(5.5) and (5.6). (ZAYOUD et al., 2022; CURTEANU, 2003) It is worth noting also that these adjusted input values as shown in Tables (5.4), (5.5) and (5.6) were applied in order to capture the stochasticity of the FRP of the styrene reaction by the HSSA. Moreso, the deviations for the polydispersity indices or PDIs for both the stochastic and deterministic recorded were reportedly minimal. However, due to the operating temperature of 140°C, the polymerization chain reaction transits to a more narrower MWD region as depicted in Figures (5.1) to (5.6). Overall, as observed for both deterministic and stochastic simulation outcomes, the PDIs shown in Tables (5.4), (5.5) and (5.6) were lesser than 1.50 which further signifies a narrower MWD thus, this implies that the polymer chains have a more uniform size or length.

Furthermore, in terms of the number-average molar mass (Mn) and weight-average molar mass (Mw), Figures (5.1) and (5.2) shows more numerical deviations for the MWD compared to the Figures (5.3) to (5.6) when comparing both the deterministic profiles and the corresponding stochastic trajectories at lower simulation times. However, the stochastic perturbations were more feasible in Figures (5.1) and (5.2) than in the Figure (5.3) through to Figure (5.4). All in all, the monomer (M) to solvent (S) ratio of 60/40 v/v compared to the other ratios used in the simulation provided a better comparative

MWD, considering the multiplicative scale factor, k and operating temperature, T. Overall, based on the conditions used to validate the HSSA in this work, it is worth noting that, the increased value of the molar concentration (mol/L) for the Monomer (M), Solvent (S) and Initiator (I) were subjected to a higher operating temperature (140°C) to accelerate the chemical reaction. This resulted in narrower molecular weight distribution (MWD) or uniformity as shown by PDIs less than a value of 1.50 which denotes improved mechanical strength, structural stability and application performance when compared to higher PDIs. SHRIVASTAVA, 2018

In summary, one of the advantages of this technique is that there is no need to complement the simulation of the FRP chemical reaction system by solving a set of stiff nonlinear ODEs or first-degree Differential Algebraic Equations (DAEs) which are obtained from the traditional Methods of Moments technique deployed in deterministic simulation approaches. (MAAFA, J. B. P. SOARES, and ELKAMEL, 2007) In order words, the mathematical modelling procedure usually deployed in FRP reaction systems involves the application of assumptions such as the Long Chain Approximation (LCA) and Quasi-Steady State Approximation (QSSA) that were not considered in this work. (MASTAN and ZHU, 2015) The HSSA used in this work is proven to be an effective tool for tracking the rate of monomer consumption and the molecular weight distributions of the growing chain of the polymer. With this technique, the feeding conditions and operating temperature can be effectively optimized to meet large-scale production expectations.

CHAPTER 6
CONCLUDING REMARKS AND FUTURE OUTLOOK

6.0.1 Concluding Remarks of Simulated Results

In this project, the FRP of styrene in microchannels (reactions in milli- or micro-reactor) was modelled by applying the HSSA. The algorithm used in this project was validated by the experiment performed by Fullin et al. (2015). Polymers are a function of reactive sites or complex radicals which affects the chain performance thus, average molecular weight distribution is not enough to control the end-use properties of the formed polymer. Therefore, it suffices to say that based of the nature of the obtained results, the HSSA provided a good prediction of the earlier experiment performed using a mill-reactor. (NASRESFAHANI and R. A. HUTCHINSON, 2018)

Furthermore, it is worth noting that, the HSSA proved to be successful in the prediction of the end-use characteristic of polystyrene such as monomer conversion rate (X), Molecular weight distribution (MWD) and, the polydispersity index (PDI) of polystyrene. However, the polymer end-use properties such as the number-average molar mass (Mn), weight-average molar mass (Mw), polydispersity indices (PDI) and monomer conversion rate (X) produced more numerical deviations when when the operating conditions different from the reference experiment were changed.

Conclusively, the HSSA can provide a solid foundation for the optimization, process intensification and scaling-up of the FRP of styrene production while maintaining the desired end-use properties of the polymer.

6.1 Future Outlook

Several research efforts are made to fully model non-linear reactions like chain growth polymerization or Free Radical Polymerization reactions to predict the end-use properties of polymers. Until now, investigations are still ongoing to develop

an algorithm that could predict both the rheological and fluid flow properties of polymeric materials as well as track other phenomena such as gel, cage and glass effects during polymerization in microchannels due to low residence time involved. (Wang and Hutchinson, 2011; Gao et al., 2020) However, with the ever-increasing experimental and mechanistic data representing various polymerization reactions as well as other non-linear complex chemical reactions, the power of "learning" this vast expanse of data can not be overemphasized. (Nguyen, Tao, and Li, 2022; Sha et al., 2021)

This set of data can be trained, validate and tested by deploying robust Machine Learning (ML) algorithms or Hybrid Neural Networks (HNN). Thus, this powerful tool could prove pivotal to unravelling polymerization reactions by splitting the problem into logical steps or data-driven workflows which is poised for streamlined industrial manufacturing in the near future. (GU et al., 2021)

Applications of simple Neural Networks (NNs) have been employed to determine conversion rates, polydispersity index, mass and number molecular weight distributions using experimental and mechanistic data from a batch reactor for the bulk Free Radical Polymerization of Methyl Methacrylate (MMA) by Curteanu et al.(2020). This simple neural network modelling methodology produced a very good representation of the bulk polymerization of MMA. (CURTEANU, 2020) Also, Neural Network (NN) topology like the multilayer perceptron (MLP) has been designed to simulate FRP of styrene, showing a very good standard deviation ratio and correlation with experimental data. (DA CUNHA, DE SOUZA, and FOLLY, 2007)

A powerful variant of a hybrid neural network is the Hybrid Stochastic Neural Network (HSNN). They can also simulate intrinsically non-linear chemical reactions, which can be applied to a range of problems with stochastic behaviour phenomena. (CAMPOS, VELLASCO, and LAZO, 2011) These variant neural networks are trained using a maximum propensity function on the posterior one-step of the density of the training data samples. (DRIDI, DRUMETZ, and FABLET, 2021) Another advantage of a robust and effective HSNN is that preliminary results obtained from learning complex dynamical reaction systems illustrate the relevance of considering a Stochastic Differentiation Equation (SDE) formulation as well as good performance in terms of Root Mean Square Error (RMSE). (DRIDI, DRUMETZ, and FABLET, 2021)

Hence, it is believed that the data obtained from FRP reactions using micro- or milli-reactors would serve effectively at both microscale (pilot experimentation) and macroscale (industrial scale). The simulation of the FRP reaction using HSNN would be robust and computationally effective to predict and control the rheological, and fluid flow properties of the end-use polymer.

6.2 Publications

Below is a publication from the thesis.

Conference Paper
Edward, U. I. , Vianna A.S.(Oct,2022). "Stochastic Modelling and Simulation of Free Radical Polymerization of Styrene in Microchannels using a Hybrid Gillespie Algorithm." *XXV National Meeting of Computational Modeling (XXV ENMC) and the XIII Meeting of Materials Science and Technology (XIII ECTM).*

Peer-Reviewed Journal
Edward, U. I., Vianna A.S.(Feb,2023). "Stochastic Modelling and Simulation of Free Radical Polymerization of Styrene in Microchannels using a Hybrid Gillespie Algorithm." *The Journal of Engineering and Exact Sciences – (jCEC).*

6.2.1 Publication(s) by DOI

Feb, 2023 **doi:10.18540/jcecvl9iss1pp15327-01e**

BIBLIOGRAPHY

ASCHER, U. M. and P. LINDA (1998). *Computer methods for ordinary differential equations and differential-algebraic equations*, pp. 3–305. DOI: 10.1137/1.9781611971392.

BAWN, C.S.H. (1987). "Encyclopedia of polymer science and engineering". In: *Polymer* 28.7, p. 1234. ISSN: 00323861. DOI: 10.1016/0032-3861(87)90274-6.

BENOIT, DIDIER et al. (2000). "Kinetics and mechanism of controlled free-radical polymerization of styrene and n-butyl acrylate in the presence of an acyclic β-phosphonylated nitroxide". In: *Journal of the American Chemical Society* 122.25, pp. 5929–5939. ISSN: 00027863. DOI: 10.1021/ja991735a.

BURKE, PAULO EDUARDO PINTO (Mar. 2021). "Simulation of biochemical systems using constraint-based methods and complex networks". In: DOI: 10.11606/T.95.2021.TDE-23032021-143111.

CABRAL, P. A. et al. (2003). *Free-Radical Solution Polymerization of Styrene in a Tubular Reactor - Effects of Recycling*. DOI: 10.1002/pen.10099. (Visited on 04/17/2022).

CAMPOS, LUCIANA C.D., MARLEY M.B.R. VELLASCO, and JUAN G.L. LAZO (2011). "A stochastic model based on neural networks". In: *Proceedings of the International Joint Conference on Neural Networks*. ISBN: 9781457710865. DOI: 10.1109/IJCNN.2011.6033399.

CAO, Y., D.T GILLESPIE, and L. PETZOLD (Feb. 2005). "The slow-scale stochastic simulation algorithm". In: *The Journal of chemical physics* 122, p. 14116. DOI: 10.1063/1.1824902.

CAO, Y., D.T. GILLESPIE, and L. R. PETZOLD (2005). "Avoiding negative populations in explicit Poisson tau-leaping". In: *Journal of Chemical Physics* 123.5. ISSN: 00219606. DOI: 10.1063/1.1992473.

CAO, Y. and L. PETZOLD (2008). "Slow-scale tau-leaping method". In: *Computer Methods in Applied Mechanics and Engineering* 197.43-44, pp. 3472–3479. ISSN: 00457825. DOI: 10.1016/j.cma.2008.02.024.

CAO, YANG, D.T. GILLESPIE, and LINDA R. PETZOLD (Jan. 2006). "Efficient step size selection for the tau-leaping simulation method". In: *Journal of Chemical Physics* 124.4, p. 044109. ISSN: 00219606. DOI: 10.1063/1.2159468.

CHATTERJEE, ABHIJIT, DIONISIOS G. VLACHOS, and MARKOS A. KATSOULAKIS (2005). "Binomial distribution based τ-leap accelerated stochastic simulation". In: *Journal of Chemical Physics* 122.2. ISSN: 00219606. DOI: 10.1063/1.1833357.

CHIEFARI, JOHN et al. (1998). "Living free-radical polymerization by reversible addition - Fragmentation chain transfer: The RAFT process". In: *Macromolecules* 31.16, pp. 5559–5562. ISSN: 00249297. DOI: 10.1021/ma9804951.

CROMPTON, T.R. (1993). "Polymer Microstructure". In: *Practical Polymer Analysis*, pp. 437–505. DOI: 10.1007/978-1-4615-2874-6_10.

CURTEANU, SILVIA (2020). "Chapter 10: Machine Learning Techniques Applied to a Complex Polymerization Process". In: *RSC Theoretical and Computational Chemistry Series*. DOI: 10.1039/9781839160233-00227.

— (2003). "Modeling and simulation of free radical polymerization of styrene under semibatch reactor conditions". In: *Central European Journal of Chemistry* 1.1, pp. 69–90. DOI: https://doi.org/10.2478/BF02479259.

CUTTER, L. A. and T. D. DREXLER (1982). "Simulation of the Kinetics of Styrene Polymerization." In: *ACS Symposium Series*, pp. 13–26. ISBN: 084120733X. DOI: 10.1021/bk-1982-0197.ch002.

DA CUNHA, FERNANDO R, MAURÍCIO B DE SOUZA, and ROSSANA O. M. FOLLY (2007). "NEURAL NETWORK-BASED PREDICTION OF POLYSTYRENE PRODUCT QUALITY FROM FREE RADICAL REACTION CONDITIONS". In.

DAGMAR, R.D et al. (Oct. 2015). "Model-based design of the polymer microstructure: Bridging the gap between polymer chemistry and engineering". In: *Polymer Chemistry* 6.40, pp. 7081–7096. ISSN: 17599962. DOI: 10.1039/c5py01069a.

— (July 2016). "The strength of multi-scale modeling to unveil the complexity of radical polymerization". In: *Progress in Polymer Science* 58, pp. 59–89. ISSN: 00796700. DOI: 10.1016/j.progpolymsci.2016.04.002.

DANIEL, COLOMBANI (1997). "Chain-growth control in free radical polymerization". In: *Progress in Polymer Science* 22.8, pp. 1649–1720. ISSN: 0079-6700. DOI: https://doi.org/10.1016/S0079-6700(97)00022-1.

DRAWERT, BRIAN et al. (Feb. 2017). "GillesPy: A Python Package for Stochastic Model Building and Simulation". In: *IEEE Life Sciences Letters* PP, pp. 1–1. DOI: 10.1109/LLS.2017.2652448.

DRIDI, NOURA, LUCAS DRUMETZ, and RONAN FABLET (2021). "Learning stochastic dynamical systems with neural networks mimicking the Euler-Maruyama scheme". In: *European Signal Processing Conference*. ISBN: 9789082797060. DOI: 10.23919/EUSIPCO54536.2021.9616068. arXiv: 2105.08449.

DUAN, Q. and J. LIU (2015). “A first step to implement Gillespie’s algorithm with rejection sampling”. In: *Statistical Methods and Applications* 24.1, pp. 85–95. ISSN: 1613981X. DOI: 10.1007/s10260-014-0283-6.

FICHTHORN, K.A. and W. H. WEINBERG (1991). “Theoretical foundations of dynamical Monte Carlo simulations”. In: *The Journal of Chemical Physics* 95.2, pp. 1090–1096. ISSN: 00219606. DOI: 10.1063/1.461138.

FLAVIO, F. et al. (2017). “Contribution of microreactor technology and flow chemistry to the development of green and sustainable synthesis”. In: *Beilstein Journal of Organic Chemistry* 13, pp. 520–542. ISSN: 1860-5397. DOI: 10.3762/bjoc.13.51. URL: https://doi.org/10.3762/bjoc.13.51.

FROUNCHI, M., FATOLA FARHADI, and R. MOHAMMADI (Jan. 2002). “Simulation of styrene radical polymerization in the batch reactor: A modified kinetic model for high conversion”. In: 9, pp. 86–92.

FU, YAO, MICHAEL F. CUNNINGHAM, and ROBIN A. HUTCHINSON (2007). “Modeling of Nitroxide-Mediated Semibatch Radical Polymerization”. In: *Macromolecular Reaction Engineering* 1.2, pp. 243–252. ISSN: 1862832X. DOI: 10.1002/mren.200600024.

FULLIN, L. et al. (2015). “Solution styrene polymerization in a millireactor”. In: *Chemical Engineering and Processing: Process Intensification* 98, pp. 1–12. DOI: 10.1016/j.cep.2015.09.017.

Gao, Yongsheng et al. (2020). *Complex polymer architectures through free-radical polymerization of multivinyl monomers*. DOI: 10.1038/s41570-020-0170-7.

GAO, ZEHUI and JUNPO HE (Oct. 2015). “Monte Carlo Modeling of Free Radical Polymerization in Microflow Reactors”. In: *Macromolecular Reaction Engineering* 9.5, pp. 431–441. ISSN: 18628338. DOI: 10.1002/mren.201400061.

GARTNER, THOMAS E. and ARTHI JAYARAMAN (2019). “Modeling and Simulations of Polymers: A Roadmap”. In: *Macromolecules* 52.3, pp. 755–786. ISSN: 15205835. DOI: 10.1021/acs.macromol.8b01836. URL: https://pubs.acs.org/sharingguidelines.

El-Ghoul, Yassine et al. (2021). “Recent advances in functional polymer materials for energy, water, and biomedical applications: A review”. In: 13.24. ISSN: 20734360. DOI: 10.3390/polym13244327.

GIBSON, M. A. and J. BRUCK (2000). “Efficient exact stochastic simulation of chemical systems with many species and many channels”. In: *Journal of Physical Chemistry A* 104.9, pp. 1876–1889. ISSN: 10895639. DOI: 10.1021/jp993732q.

GILLESPIE, D.T. (Dec. 1976). “A general method for numerically simulating the stochastic time evolution of coupled chemical reactions”. In: *Journal of Computational Physics* 22.4, pp. 403–434. ISSN: 10902716. DOI: 10.1016/0021-9991(76)90041-3.

GILLESPIE, D.T. (July 2001). “Approximate accelerated stochastic simulation of chemically reacting systems”. In: *Journal of Chemical Physics* 115.4, pp. 1716–1733. ISSN: 00219606. DOI: 10.1063/1.1378322.

— (1977). “Exact stochastic simulation of coupled chemical reactions”. In: *Journal of Physical Chemistry* 81.25, pp. 2340–2361. ISSN: 00223654. DOI: 10.1021/j100540a008.

— (Apr. 2007). “Stochastic simulation of chemical kinetics”. In: *Annual Review of Physical Chemistry* 58, pp. 35–55. ISSN: 0066426X. DOI: 10.1146/annurev.physchem.58.032806.104637.

GU, YU et al. (2021). “Machine learning-assisted systematical polymerization planning: case studies on reversible-deactivation radical polymerization”. In: *Science China Chemistry*. ISSN: 18691870. DOI: 10.1007/s11426-020-9969-y.

HAHL, SAYURI K. and ANDREAS KREMLING (Aug. 2016). “A comparison of deterministic and stochastic modeling approaches for biochemical reaction systems: On fixed points, means, and modes”. In: *Frontiers in Genetics* 7, p. 157. ISSN: 16648021. DOI: 10.3389/fgene.2016.00157.

HASELTINE, ERIC L. and JAMES B. RAWLINGS (2002). “Approximate simulation of coupled fast and slow reactions for stochastic chemical kinetics”. In: *Journal of Chemical Physics* 117.15, pp. 6959–6969. ISSN: 00219606. DOI: 10.1063/1.1505860.

HIDETAKA, TOBITA (2015). “Model-based reactor design in free-radical polymerization with simultaneous long-chain branching and scission”. In: *Processes* 3.4, pp. 731–748. ISSN: 22279717. DOI: 10.3390/pr3040731.

HIGHAM, DESMOND J. (2008). “Modeling and simulating chemical reactions”. In: *SIAM Review* 50.2, pp. 347–368. ISSN: 00361445. DOI: 10.1137/060666457.

HONG, KUNLUN et al. (Aug. 2002). “Conventional free radical polymerization in room temperature ionic liquids: A green approach to commodity polymers with practical advantages”. In: *Chemical communications (Cambridge, England)* 13, pp. 1368–9. DOI: 10.1039/b204319j.

HSSA, WIKIPEDIA (2022). *Hybrid stochastic simulation - Wikipedia*. URL: https://en.wikipedia.org/wiki/Hybrid_stochastic_simulation (visited on 08/21/2022).

HUI, ALBERT W. and ARCHIE E. HAMIELEC (1972). “Thermal polymerization of styrene at high conversions and temperatures. An experimental study”. In: *Journal of Applied Polymer Science* 16.3, pp. 749–769. ISSN: 10974628. DOI: 10.1002/app.1972.070160319.

IWUCHUKWU, E.U and A.S.J VIANNA (2023). “Stochastic Modelling and Simulation of Free Radical Polymerization of Styrene in Microchannels using a Hybrid Gillespie Algorithm”. In: *The Journal of Engineering and Exact Sciences* 9.1, 15327–01e.

Jafarzadeh-Kashi, Tahereh Sadat et al. (2011). “Polymerization behavior and thermal characteristics of two new composites at five temperatures: Refrigeration to

preheating". In: *Journal of Advanced Prosthodontics* 3.4, pp. 216–220. ISSN: 20057806. DOI: 10.4047/jap.2011.3.4.216.

JÄHNISCH, KLAUS et al. (2004). "Chemistry in Microstructured Reactors". In: *Angewandte Chemie - International Edition* 43.4, pp. 406–446. ISSN: 14337851. DOI: 10.1002/anie.200300577.

JAISWAL, P. et al. (2022). "Covalently Immobilized Nickel Nanoparticles Reinforce Augmentation of Mass Transfer in Millichannels for Two-Phase Flow Systems". In: *Industrial & Engineering Chemistry Research* 61.10, pp. 3672–3684. DOI: 10.1021/acs.iecr.1c04419. URL: https://doi.org/10.1021/acs.iecr.1c04419.

KATO, MITSURU et al. (1995). *Polymerization of Methyl Methacrylate with the Carbon Tetrachloride/Dichlorotris-(triphenylphosphine)ruthenium(II)/ Methylaluminum Bis(2,6-di-tert-butylphenoxide) Initiating System: Possibility of Living Radical Polymerization*. DOI: 10.1021/ma00109a056.

KIM, K. J. and K. Y. CHOI (1989). "Modeling of free radical polymerization of styrene catalyzed by unsymmetrical bifunctional initiators". In: *Chemical Engineering Science* 44.2, pp. 297–312. ISSN: 00092509. DOI: 10.1016/0009-2509(89)85066-3.

KUMAR, Y. et al. (2022). "A critical review on nanoparticle-assisted mass transfer and kinetic study of biphasic systems in millimeter-sized conduits". In: *Chemical Engineering and Processing - Process Intensification* 170, p. 108675. ISSN: 0255-2701. DOI: https://doi.org/10.1016/j.cep.2021.108675. URL: https://www.sciencedirect.com/science/article/pii/S0255270121003639.

LAURENCE, R. L., R. GALVAN, and M. V. TIRRELL (1994). "Mathematical modelling of polymerization kinetics". In: *Polymer Reactor Engineering*, pp. 87–124. DOI: 10.1007/978-94-011-1338-0_3.

MAAFA, IBRAHIM M., JOÃO B. P. SOARES, and ALI ELKAMEL (2007). "Prediction of Chain Length Distribution of Polystyrene Made in Batch Reactors with Bifunctional Free-Radical Initiators Using Dynamic Monte Carlo Simulation". In: *Macromolecular Reaction Engineering* 1.3, pp. 364–383. DOI: https://doi.org/10.1002/mren.200700007.

Martin, Tyler B. and Debra J. Audus (2023). *Emerging Trends in Machine Learning: A Polymer Perspective*. DOI: 10.1021/acspolymersau.2c00053.

MASON, D. R., T. S. HUDSON, and A. P. SUTTON (2005). "Fast recall of state-history in kinetic Monte Carlo simulations utilizing the Zobrist key". In: *Computer Physics Communications* 165.1, pp. 37–48. ISSN: 00104655. DOI: 10.1016/j.cpc.2004.09.007.

MASTAN, ERLITA and SHIPING ZHU (July 2015). "Method of moments: A versatile tool for deterministic modeling of polymerization kinetics". In: *European Polymer Journal* 68.68, pp. 139–160. ISSN: 00143057. DOI: 10.1016/j.eurpolymj.2015.04.018.

MATYJASZEWSKI, KRZYSZTOF and SCOTT G. GAYNOR (2000). "FREE RADICAL POLYMERIZATION". In: ed. by Clara D. Craver and Charles E. Carraher, pp. 929–977. DOI: https://doi.org/10.1016/B978-008043417-9/50046-5. URL: https://www.sciencedirect.com/science/article/pii/B9780080434179500465.

MAVRANTZAS, V.G. (2021). "Using Monte Carlo to Simulate Complex Polymer Systems: Recent Progress and Outlook". In: 9. ISSN: 2296424X. DOI: 10.3389/fphy.2021.661367.

MEIMAROGLOU, DIMITRIOS and COSTAS KIPARISSIDES (June 2014). "Review of Monte Carlo methods for the prediction of distributed molecular and morphological polymer properties". In: *Industrial and Engineering Chemistry Research* 53.22, pp. 8963–8979. ISSN: 15205045. DOI: 10.1021/ie4033044.

MENDEZ-PORTILLO, LIONEL SERGIO (2011). "Free-Radical Polymerization of Polystyrene Using Microreaction Technology". In: *Chemical Engineering*, pp. 1–231. URL: https://publications.polymtl.ca/551/.

MILLS, P.L., DAVID J.Q, and F.R JAMES (2007). "Microreactor technology and process miniaturization for catalytic reactions-A perspective on recent developments and emerging technologies". In: *Chemical Engineering Science* 62.24, pp. 6992–7010. ISSN: 00092509. DOI: 10.1016/j.ces.2007.09.021.

MOAD, G. (2016). "Radical Polymerization". In: *Reference Module in Materials Science and Materials Engineering*. Elsevier. ISBN: 978-0-12-803581-8. DOI: https://doi.org/10.1016/B978-0-12-803581-8.01346-1.

NAOYA, HASHIMOTO (2019). "Emulsifiers for Emulsion Polymerization". In: 513, pp. 1–4.

NASRESFAHANI, A. and R. A. HUTCHINSON (2018). "Modeling the Distribution of Functional Groups in Semibatch Radical Copolymerization: An Accelerated Stochastic Approach". In: *Industrial and Engineering Chemistry Research*. ISSN: 15205045. DOI: 10.1021/acs.iecr.8b01943.

NESVADBA, PETER (2012). "Encyclopedia of radicals in chemistry, biology and materials". In: 49.11, pp. 49–6017–49–6017. ISSN: 0009-4978. DOI: 10.5860/choice.49-6017.

Nguyen, Danh, Lei Tao, and Ying Li (2022). "Integration of Machine Learning and Coarse-Grained Molecular Simulations for Polymer Materials: Physical Understandings and Molecular Design". In: *Frontiers in Chemistry* 9. ISSN: 22962646. DOI: 10.3389/fchem.2021.820417.

Nising, Philip (2006). "High-Temperature Radical Polymerization of Methyl Methacrylate in a Continuous Pilot Scale Process". PhD thesis.

ODIAN, G. (2004). *Principles of Polymerization, 4th Edition*. ISBN: 978-0-471-27400-1. eprint: arXiv:1011.1669v3.

RATHINAM, M. et al. (2003). “Stiffness in stochastic chemically reacting systems: The implicit tau-leaping method”. In: *Journal of Chemical Physics* 119.24, pp. 12784–12794. ISSN: 00219606. DOI: 10.1063/1.1627296.

Rego, Diogo et al. (Apr. 2020). “Innovations in Polymer Applications - Plastic Packaging”. In: *Journal of Research Updates in Polymer Science* 9, pp. 24–31. DOI: 10.6000/1929-5995.2020.09.02.

RESHNIAK, VIKTOR, ABDUL KHALIQ, and DAVID VOSS (2019). “Slow-scale split-step tau-leap method for stiff stochastic chemical systems”. In: *Journal of Computational and Applied Mathematics* 361, pp. 79–96. ISSN: 03770427. DOI: 10.1016/j.cam.2019.03.044.

SERRA, CHRISTOPHE (2013). *Free Radical Polymerization*. Vol. 2. American Chemical Society Division of Polymeric Materials: Science and Engineering, pp. 197–212. ISBN: 9783527315505. DOI: 10.1002/9783527631445.ch29. URL: http://dx.doi.org/10.1016/B978-0-08-043417-9.50046-5.

SEYEDI, ALI et al. (2020). “Initiator Feeding Policies in Semi-Batch Free Radical Polymerization: A Monte Carlo Study”. In: *Processes* 8.10. ISSN: 2227-9717. DOI: 10.3390/pr8101291. URL: https://www.mdpi.com/2227-9717/8/10/1291.

Sha, Wuxin et al. (2021). *Machine learning in polymer informatics*. DOI: 10.1002/inf2.12167.

SHAO, JING et al. (2015). “Monte Carlo simulation on the kinetics of batch and semi-batch free radical polymerization”. In: *Macromolecular Research* 23.11, pp. 1042–1050. ISSN: 20927673. DOI: 10.1007/s13233-015-3136-8.

SHRIVASTAVA, ANSHUMAN (2018). “2 - Polymerization”. In: *Introduction to Plastics Engineering*. Ed. by Anshuman Shrivastava. Plastics Design Library. William Andrew Publishing, pp. 17–48. ISBN: 978-0-323-39500-7. DOI: https://doi.org/10.1016/B978-0-323-39500-7.00002-2.

SHUSAKU, A. et al. (2017). “Precise analysis and control of polymerization kinetics using a microflow reactor”. In: *Chemical Engineering and Processing: Process Intensification* 119, pp. 73–80. ISSN: 02552701. DOI: 10.1016/j.cep.2017.05.016.

SLEPOY, A., A.P. THOMPSON, and S.J. PLIMPTON (2008). “A constant-time kinetic Monte Carlo algorithm for simulation of large biochemical reaction networks”. In: *Journal of Chemical Physics* 128.20. ISSN: 00219606. DOI: 10.1063/1.2919546.

SMITH, G.D. (2007). “Modeling the Stochastic Gating of Ion Channels”. In: *Computational Cell Biology*, pp. 285–319. DOI: 10.1007/978-0-387-22459-6_11.

SOARES, J.B.P. (2004). *Polyolefins with Long Chain Branches Made with Single-Site Coordination Catalysts: A Review of Mathematical Modeling Techniques for Polymer Microstructure*. DOI: 10.1002/mame.200300350.

SOSNOWSKI, STANISLAW and RYSZARD SZYMANSKI (2022). “Living polymerization in nano-scale volumes. Impact of process conditions on polymerization kinetics and product characteristics”. In: *Chemical Engineering Journal* 449, p. 137729.

ISSN: 1385-8947. DOI: https://doi.org/10.1016/j.cej.2022.137729. URL: https://www.sciencedirect.com/science/article/pii/S1385894722032168.

STAMATAKIS, M. and D.G. VLACHOS (2012). "Unraveling the complexity of catalytic reactions via kinetic Monte Carlo simulation: current status and frontiers". In: *Acs Catalysis* 2.12, pp. 2648–2663.

STANISLAW, SOSNOWSKI and SZYMANSKI RYSZARD (2019). "A novel efficient hybrid algorithm for Monte Carlo simulation of controlled radical polymerization: The method integrating reactive and deactivated species". In: *Chemical Engineering Journal* 358.July 2018, pp. 197–210. ISSN: 13858947. DOI: 10.1016/j.cej.2018.09.154. URL: https://doi.org/10.1016/j.cej.2018.09.154.

STUART, MARTIEN A. COHEN et al. (2010). "Emerging applications of stimuli-responsive polymer materials". In: *Nature materials* 9.2, pp. 101–113.

SU, Y., Y. SONG, and L. XIANG (2018). "Continuous-Flow Microreactors for Polymer Synthesis: Engineering Principles and Applications". In: 376.6. ISSN: 23648961. DOI: 10.1007/s41061-018-0224-1. (Visited on 01/07/2022).

TEUSCHEL, U. (2001). *What is a microreactor? It is a miniature version of the traditional, large-scale reactor that most people are familiar with.* DOI: 10.1016/S1389-0352(01)00045-9.

THANH, V.H, C. PRIAMI, and R. ZUNINO (2014). "Efficient rejection-based simulation of biochemical reactions with stochastic noise and delays". In: *Journal of Chemical Physics* 141.13. ISSN: 10897690. DOI: 10.1063/1.4896985.

TIAN, T. and K. BURRAGE (2004). "Binomial leap methods for simulating stochastic chemical kinetics". In: *Journal of Chemical Physics* 121.21, pp. 10356–10364. ISSN: 00219606. DOI: 10.1063/1.1810475.

TOBITA, HIDETAKA (Sept. 1996). *Kinetics of free-radical polymerization with chain-length-dependent bimolecular termination under unstationary conditions.* Tech. rep., pp. 3073–3080. DOI: 10.1021/ma9512871.

Tobita, Hidetaka (1998). "Markovian approach to nonlinear polymer formation: Free-radical polymerization with chain transfer to polymer". In: *Journal of Polymer Science, Part B: Polymer Physics* 36.2, pp. 357–371. ISSN: 08876266. DOI: 10.1002/(SICI)1099-0488(19980130)36:2<357::AID-POLB14>3.0.CO;2-G.

TRIGILIO, ALESSANDRO D. et al. (2020). "Gillespie-Driven kinetic Monte Carlo Algorithms to Model Events for Bulk or Solution (Bio)Chemical Systems Containing Elemental and Distributed Species". In: *Industrial & Engineering Chemistry Research* 59.41, pp. 18357–18386. DOI: 10.1021/acs.iecr.0c03888.

TRIPATHI, AMIT K. and DONALD C. SUNDBERG (2015). "A hybrid algorithm for accurate and efficient Monte Carlo simulations of free-radical polymerization reactions". In: *Macromolecular Theory and Simulations* 24.1, pp. 52–64. ISSN: 15213919. DOI: 10.1002/mats.201400062.

VIANNA Jr., A.S. et al. (2007). “A stochastic flow model for a tubular solution polymerization reactor”. In: *Polymer Engineering and Science* 47.11, pp. 1839–1846. ISSN: 15482634. DOI: 10.1002/pen.20893.

VIANNA JR., ARDSON DOS SANTOS (2003). “TUBULAR POLYMERIZATION REACTORS: FLUID DYNAMIC CHARACTERIZATION, MODELLING AND SIMULATION”. PhD Dissertation. Universidade Federal do Rio de Janeiro(UFRJ).

VICEVIC, MARIJA, KATARINA NOVAKOVIC, and KAMELIA BOODHOO (2021). “Free-Radical Polymerization of Styrene: Kinetic Study in a Spinning Disc Reactor (SDR)”. In: *Frontiers in Chemical Engineering* 3. DOI: 10.3389/fceng.2021.661498.

VIEIRA, RONIÉRIK PIOLI and LILIANE MARIA FERRARESO LONA (Oct. 2016). “Simulation of temperature effect on the structure control of polystyrene obtained by atom-transfer radical polymerization”. In: *Polímeros* 26.4, pp. 313–319. ISSN: 0104-1428. DOI: 10.1590/0104-1428.2376.

VOLKER, HESSEL, LÖWE HOLGER, and SCHÖNFELD FRIEDHELM (2005). “Micromixers—a review on passive and active mixing principles”. In: *Chemical Engineering Science* 60.8. 5th International Symposium on Mixing in Industrial Processes (ISMIP5), pp. 2479–2501. ISSN: 0009-2509. DOI: https://doi.org/10.1016/j.ces.2004.11.033. URL: https://www.sciencedirect.com/science/article/pii/S0009250904009364.

Wang, Wei and Robin A. Hutchinson (2011). “A comprehensive kinetic model for high-temperature free radical production of styrene/methacrylate/acrylate resins”. In: *AIChE Journal* 57.1, pp. 227–238. ISSN: 00011541. DOI: 10.1002/aic.12258.

WARD, I.M. (2009). “Polymers: Chemistry and Physics of Modern Materials, 3rd edition, by J.M.G. Cowie and V. Arrighi”. In: *Contemporary Physics* 50.6, pp. 670–670. ISSN: 0010-7514. DOI: 10.1080/00107510902992270.

WILLE, CH et al. (2004). “Synthesis of pigments in a three-stage microreactor pilot plant—an experimental technical report”. In: *Chemical Engineering Journal* 101.1. 7th International Conference on Microreaction Technology, pp. 179–185. ISSN: 1385-8947. DOI: https://doi.org/10.1016/j.cej.2003.11.007. URL: https://www.sciencedirect.com/science/article/pii/S1385894703003152.

XEROXCORP (2003). *Stable Free Radical Polymerization*. URL: https://web.archive.org/web/20031128090841/http://www.xeroxtechnology.com/sfrp.

YAO, XINGJUN et al. (2015). *Review of the applications of microreactors*. DOI: 10.1016/j.rser.2015.03.078.

ZAYOUD, AZD et al. (2022). “Pyrolysis of end-of-life polystyrene in a pilot-scale reactor: Maximizing styrene production”. In: *Waste Management* 139, pp. 85–95. ISSN: 18792456. DOI: 10.1016/j.wasman.2021.12.018.